



Influence of hydro-climatic factors on future coastal land susceptibility to erosion in Bangladesh: a geospatial modelling approach

Asib Ahmed^{1,2} · Rizwan Nawaz¹ · Clare Woulds¹ · Frances Drake¹

Published online: 20 April 2020
© The Author(s) 2020

Abstract

This study envisaged the likely impacts of future hydro-climatic changes on the susceptibility of coastal land to erosion through the development of raster-based geographical information system (GIS) model called land susceptibility to coastal erosion (LSCE). The model was applied to the coastal area of Bangladesh to assess future erosion susceptibility under four greenhouse gas (GHG) concentration trajectories: A1B, RCP2.6, RCP4.5 and RCP8.5. The results indicate considerable changes in future scenarios of coastal land susceptibility to erosion in the area compared to current baseline conditions. The current area of 276.33 km² (0.61%) high and very high susceptible lands would be substantially increased to 1019.13 km² (2.25% of land), 799.16 km² (1.77%), 1181.38 km² (2.61%) and 4040.71 km² (8.96%) by 2080 under A1B, RCP2.6, RCP4.5 and RCP8.5 scenarios, respectively. Spatially, the western and eastern coastal zones would have low to moderate susceptibility to erosion, whereas the central coastal zone would have moderate to high/very high susceptibility to erosion. Seasonally, the model predicted the high erosion susceptibility during the monsoon seasons and very low erosion susceptibility during the winter seasons in the future. The model outputs were enhanced by integrating experts' judgements through fuzzy cognitive mapping (FCM) approach. The LSCE model might be indispensable for coastal researchers in generating future scenarios of physical susceptibility to erosion for highly dynamic coastal areas around the world.

Keywords Climate · Erosion · LSCE · Susceptibility

Introduction

Along with a number of coastal hazards such as tidal surge, cyclone, flooding, the excessive rate of coastal erosion considerably increases coastal vulnerability at national, regional and global levels (Ramieri et al. 2011). Coastal erosion is the result of natural factors (e.g. sea level rise, wave actions, etc.)

and human actions (e.g. engineering works, land reclamation, deforestation, etc.) (Alexandrakis et al. 2010; Van 2011). Coastal susceptibility to erosion, however, designates the degree of physical resistance of coastal lands to erosion. Susceptibility to erosion essentially derives from physical forces and often can largely be treated as independent of human influences (United Nations Development Programme (UNDP) 2004). Along with a number of predispositions and preparatory factors, a range of triggering factors such as heavy rainfall, sea level rise, prevailing winds and discharge of water govern the likelihood and severity of susceptibility to erosion (Saunders and Glassey 2007; MPI 2017). These triggering factors are closely associated with changes in climatic conditions. However, there is a growing interest in the scientific community about the response of shorelines to the changes in future climate (Naylor et al. 2010). The likely changes in future climate might have substantial influences on triggering factors (MPI 2017), the consequent results of which would convert a considerable amount of coastal lands into high erosion susceptibility. For instance, future scenarios of sea level rise might change the horizontal configuration of all coastlines

✉ Asib Ahmed
asib01geo@du.ac.bd

Rizwan Nawaz
n.r.nawaz@leeds.ac.uk

Clare Woulds
c.woulds@leeds.ac.uk

Frances Drake
f.drake@leeds.ac.uk

¹ School of Geography, University of Leeds, Leeds LS2 9JT, UK

² Department of Geography and Environment, University of Dhaka, Dhaka, Bangladesh

(Warrick and Ahmad 1996; Huq et al. 1999) leading to long-term erosion of coastal lands (Fitzgerald et al., 2008). However, coastal responses to climate change are strongly determined by the site-specific factors (Masselink and Russell 2013), and hence, it is important to address the ways the underlying physical elements of any coastal system react with, and control, changes to hydro-climatic drivers.

The changes in hydro-climatic triggering factors due to global warming and consequent sea level rise are visible in the coastal area of Bangladesh (Mahmood 2012; Brown et al. 2018). Hence, it is essential for coastal researchers to synthesise the likely influences of future hydro-climatic changes on erosion susceptibility in the coastal area of the country. It is also crucial to consider the probable responses of physical settings of the coastal area to the future scenarios of those changes. Considering the mentioned situations, the current study focused on the research question: how levels of future erosion susceptibility in the coastal area of Bangladesh will undergo changes due to likely changes in hydro-climatic triggering factors? This study aimed to generate future scenarios for erosion susceptibility in the coastal area by applying the land susceptibility to coastal erosion (LSCE) model (Ahmed et al. 2018b) under the four greenhouse gas emission trajectories: A1B, RCP2.6, RCP4.5 and RCP8.5 for the three time-slices (i.e. 2020, 2050 and 2080). This is the first study to address the future impacts of hydro-climatic changes on erosion susceptibility for both the offshore and inland coastal areas of the country. The study also identified the extent of seasonal variations compared to the overall scenarios of physical susceptibility to erosion. The findings reported here for Bangladesh provide insights into how erosion along similar dynamic coastal systems around the world may respond to future hydro-climatic changes.

Methodology

Study area

Both inland and offshore coastal areas of Bangladesh were selected to apply the LSCE model in assessing future erosion susceptibility. This encompassed a land area of 45,220 km². The inland coastal limit was based on tidal movements in the area that varies between three geomorphologically distinct coastal zones: western, central and eastern (MoEF 2007; Shibly and Takewaka 2012) (Fig. 1). The variations in tidal movements are visible during different seasons. Considering the settings, this research used spectral signatures obtained from multi-temporal satellite images as a common boundary between land and water (Ahmed et al. 2018a).

This study considered the probable changes in future hydro-climatic conditions a key reason in choosing the highly dynamic coastal area of Bangladesh (Ahmed et al. 2018a) as a

case to generate future land susceptibility to erosion by applying the LSCE model. The coastal area is likely to be affected severely by the future changes in hydro-climatic conditions (Centre for Environmental and Geographic Information Services (CEGIS) 2014; BMD 2016; Climate Change Knowledge Portal (CCKP) 2016). The impacts are already visible in the coastal area of the country (Ali et al. 2007; Islam 2008). Figure 1 illustrates the likely impacts of future hydro-climatic changes in the area. The RCP4.5 rainfall scenario for monsoon season indicates a considerable increase in the total amount of rainfall in the central and eastern coastal areas of the country by 2080 (CCKP 2016). Whereas, a 1 m rise in mean sea level may inundate almost the entire exposed coastal area of the country (23,935 km²) (CEGIS 2014). The funnel-shaped coastal area is also exposed to future cyclonic storms that already affected by a number of historic tropical cyclones and strong winds (e.g. up to 260 km/h during cyclone SIDR in 2007) and storm surges (BMD 2016; Banglapedia 2018). It is predicted that the shoreline and river mouths might be pushed inland by the rising trends of Mean Sea Level (MSL) that would alter the amounts of river water discharge in the coastal area. Furthermore, the tidal range might be increased by the non-linear effect of inundation through rising sea level that could accelerate the rate of erosion in future (Huq et al. 1999; BWDB 2016; BIWTA 2017). Additionally, the occurrences of cyclones might increase in the area due to the probable changes in future climate (BMD, 2016). Moreover, the predicted rise in monsoon rainfall might increase the runoff and sediment loads in the Ganges-Brahmaputra-Meghna (GBM) river catchment area (Brammer 2014). With this, the behaviour of waves in the Bay of Bengal will affect the net landward transport of sediments (Viles and Spencer 1995). The mentioned scenarios might make the coastal area more dynamic in future.

Methods

This study assumed that there would be significant influences of hydro-climatic changes on future land susceptibility to erosion in the coastal area. A raster GIS-based model—the Land Susceptibility to Coastal erosion (LSCE)—was developed (Ahmed et al. 2018b) to assess existing susceptibility to erosion in the coastal area of Bangladesh. However, the assumption of the present study is supported by the LSCE model in which five underlying physical elements (i.e. surface elevation, surface geology, bathymetry, soil permeability and distance from shoreline) and four hydro-climatic triggering factors (i.e. discharge of coastal river water, mean sea level (MSL), rainfall and wind speed and direction) were considered as model parameters. The parameters were identified by conducting an in-depth review of the literature for the study area.

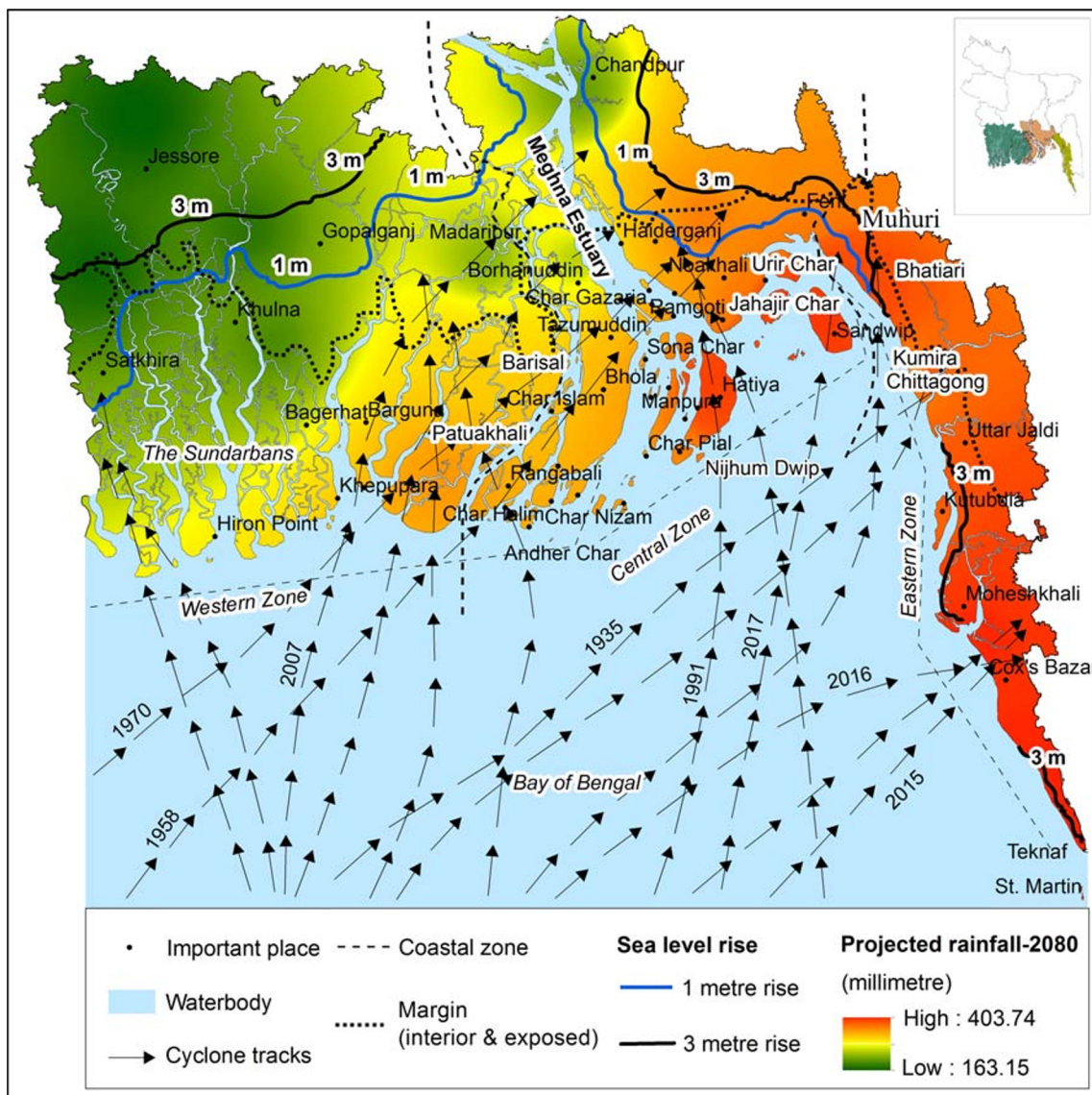


Fig. 1 The extent of the coastal area of Bangladesh selected for the present study. The figure shows the projected amount of rainfall by 2080 and the likely propagation of mean sea level under 1 m and 3 m rises. The projections of mean sea level rise show the substantial extent of land inundation in the area. Moreover, the figure shows the historical

cyclone tracts in the Bay of Bengal and the landfall places in the coastal area (data sources: BBS 2015 and BWDB 2016 (important place); CEGIS 2014 (sea level rise); CCKP 2016 (projected rainfall); MoEF 2016 (coastal zones and margin between interior and exposed coast))

To address the effects of sedimentation (accretion) and human activities (defence structures) on erosion susceptibility, this study used two sets of buffer zones known as moderators. The existing underlying physical elements were assumed as static parameters in the model for generating future scenarios of erosion susceptibility. However, future changes in the four hydro-climatic triggering factors were calculated by applying the changes in percentages of future hydro-climatic scenarios obtained from secondary sources.

The validated outputs of existing conditions (Ahmed et al. 2018b) were used as a baseline to generate future scenarios of erosion susceptibility by applying 10-year average model projections under four emission trajectories: A1B (business-as-

usual scenario), RCP2.6 (Representative Concentration Pathway-low scenario), RCP4.5 (moderate scenario) and RCP8.5 (high scenario) for three time-slices: 2020 (2015~2025), 2050 (2045~2055) and 2080 (2075~2085). By using the ‘Model Builder’ extension in ArcMap (version 10.3), the final outline of the model was designed. The ‘weighted sum’ operation in ArcMap was used to overlay the generated hydro-climatic raster surfaces on the raster surfaces prepared for existing underlying physical elements. Moreover, the impact of human activities on baseline and future land susceptibility to erosion were assessed in the present study in two ways. First, the LSCE model used defence moderators to identify the impacts of embankment, polder and

land reclamation projects. Second, a panel of experts assessed a number of potential human interventions by using fuzzy cognitive maps (FCMs), which then justified with the model parameters.

To assign weights to individual parameters, this study incorporated the opinions and ratings of 11 relevant experts having in-depth local knowledge on the selected parameters by arranging a workshop (Ahmed et al. 2018b). The weights ranged from 0 to 1 where 0 indicates no weight and 1 indicates the full weight of any parameter. The experts suggested full weights to the underlying physical elements (1 in a range of 0 to 1) for both baseline and future scenarios of the parameters. On the other hand, the weights of the hydro-climatic drivers varied: 0.84 for discharge of coastal river water; 0.79 for mean sea level; 0.71 for rainfall and 0.65 for wind speed and direction that were applied for baseline conditions and assumed to be same for future scenarios. The raster surfaces were multiplied by their given weights and finally summed together (Fig. 3).

The weighted sum scores of each scenario were then converted into five different categories starting from 0 to 100 (where 0–20 = very low (1); 21–40 = low (2); 41–60 = moderate (3); 61–80 = high (4) and 81–100 = very high (5) susceptibility to erosion). The study area embraces four prevailing seasons: winter (December to February), pre-monsoon (March to May), monsoon (June to September) and post-monsoon (October to November) (BMD 2016). Due to the scarcity of seasonal hydro-climatic scenario data, this study used only A1B trajectory-based data to generate scenarios of seasonal variation of erosion susceptibility in the coastal area. The outputs of the future scenarios were justified by incorporating the opinions of experts through fuzzy cognitive mapping (FCM).

Data sources

The baseline data for underlying physical elements were obtained from different sources (Ahmed et al. 2018b), including:

1. ASTER-DEM (Advanced Space-born Thermal Emission and Reflection Radiometer-Digital Elevation Model) from United States Geological Survey (USGS 2017) for surface elevation
2. Near-shore bathymetry from Global Multi-Resolution Topography (GMRT 2017)
3. Surface geology from United States Geological Survey (USGS 2001)
4. Soil permeability from Bangladesh Agricultural Research Council (BARC 2017)

Tide-synchronous Landsat satellite images (OLI_TIRS sensor) were collected in 2016 and used to identify the existing shoreline (considered as a mark of the mean high-

water line) for measuring distances of each pixel from the shoreline (Ahmed et al. 2018b). However, hydro-climatic data for baseline conditions were collected from different sources (BMD 2016; BWDB 2016; BIWTA 2017; PSMSL 2017; UHSLC 2017) in which long-term averages of past datasets (i.e. 1985 to 2015 for MSL, rainfall and wind speed and direction and 1995 to 2015 for water discharge) were considered. Except for water discharge, the ranges of baseline data (i.e. long-term averages) were similar to the baseline data used for hydro-climatic scenarios in the present study. Data on mean sea level were collected from six coastal stations located at Char Chenga, Chittagong, Cox's Bazar, Hiron Point, Khepupara and Sandwip. A total of 18 coastal stations were considered for the data on rainfall and wind speed and direction (the average values collected from Chittagong-IPA and Chittagong-Ambagan stations were considered as Chittagong station) whereas, 11 stations were considered for the data on discharge of coastal river water.

This study applied A1B, RCP2.6, RCP4.5 and RCP8.5 trajectory-based (IPCC 2007a, b, 2014) hydro-climatic scenario data collected from different sources (Table 1) to generate four future scenarios of land susceptibility to erosion in the coastal area. To prepare model data on future scenarios of hydro-climatic parameters, the baseline data were recalculated by using the percentage changes of parameters obtained from the model scenarios for the three time-slices. The overviews of annual average hydro-climatic data used for generating future scenarios of erosion susceptibility are presented in the Fig. 2 and Table 2.

Data processing and scaling of raster surfaces

To prepare raster surfaces, the raw data obtained for the underlying physical elements went through some pre-processing as well as some post-processing using ArcMap and Erdas Imagine software (see Fig. 3). Likewise, raster surfaces for baseline and future scenarios of the four hydro-climatic triggering factors were generated from the collected point data by applying suitable surface interpolation techniques such as inverse distance weighting (IDW) and kriging in ArcMap. However, three sets of accretion moderators were generated for baseline conditions in which a negative value (−3) was applied for the first set considering 200 m landward from the shoreline, followed by (−2) and (−1) value for 100 m and 50 m landward respectively next to the first buffer zone. To assess human interventions, (−5) was assigned to a hard defence such as a sea-wall, dyke, etc. whereas, a negative value (−3) was set for soft defences such as polder, embankments, etc. The values of the related pixels were then recalculated using 'raster calculator' tool in ArcMap that substantially reduced the previous values of the relevant pixels.

Due to uncertainties pertaining to the future areas for sedimentation and defence structures, the future

Table 1 The nature and sources of data used for future hydro-climatic scenarios in the model

LSCE model parameter	Climate scenario	Model used	Area	Source
Water discharge	A1B, RCPs	Artificial neural network (ANN)	Ganges-Brahmaputra-Meghna basin	Kamal et al. 2013
Mean sea level	A1B, RCPs	POLCOMS (Proudman Oceanographic Laboratory Coastal Ocean Modelling System) CMIP5	Coastal and shelf areas in Bangladesh Haldia station in Bay of Bengal region	Kay et al. 2015 IPCC’s AR5 report (IPCC 2014)
Rainfall	A1B, RCPs	PRECIS (Providing Regional Climate for Impact Studies) HadCM3Q regional climate model cesm1_cam5	Coastal area of Bangladesh Coastal area of Bangladesh	Institute of Water and Flood Management (IWFM 2012) Climate Change Knowledge Portal of World Bank Group (CCKP 2016)
Wind speed	A1B, RCPs	PRECIS HadCM3Q regional climate model REM02009 (MPI)	Coastal area of Bangladesh Coastal area of Bangladesh	Institute of Water and Flood Management (IWFM 2012) Centre for Climate Change Research (CCCR 2016)

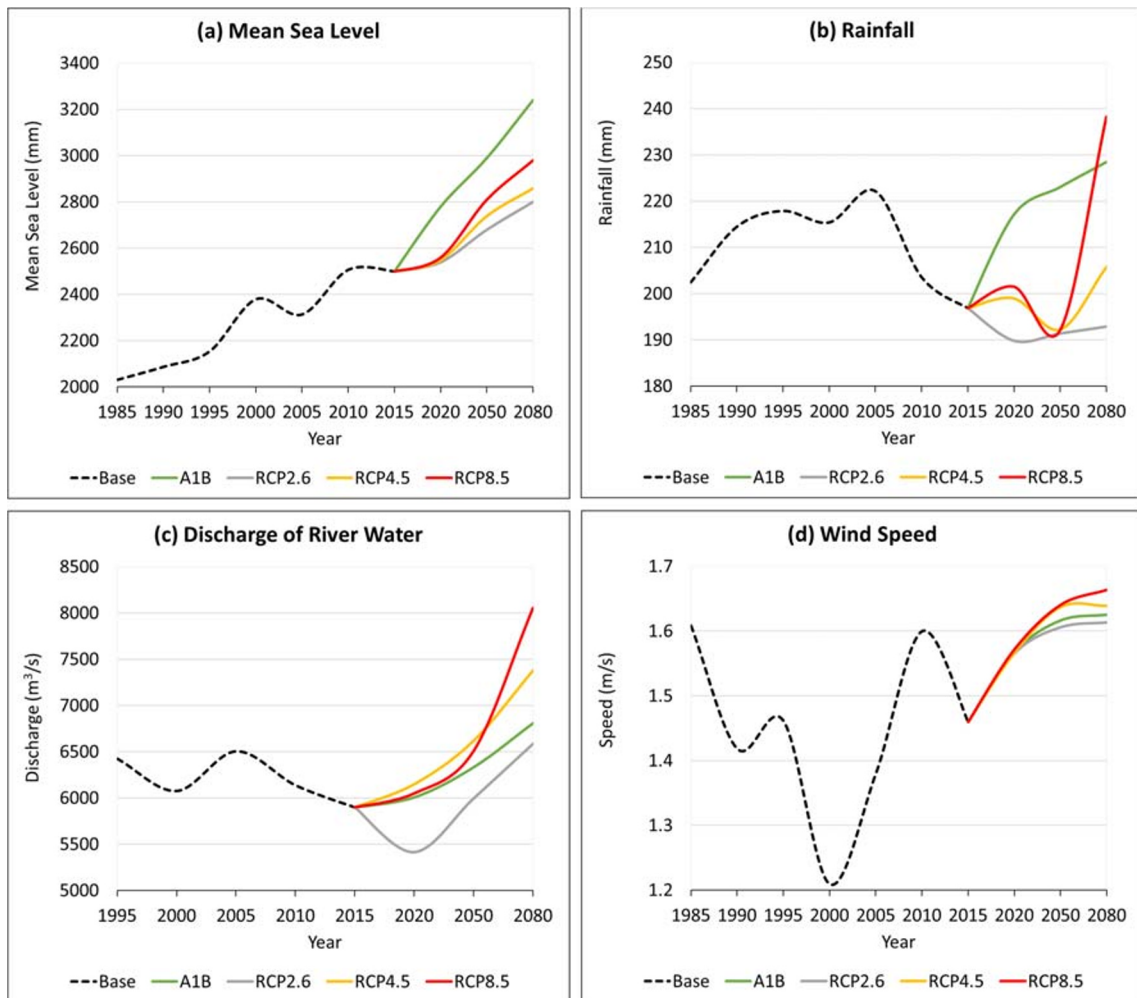


Fig. 2 Future drivers of change: (a) mean sea level; (b) rainfall; (c) discharge of river water and (d) wind speed obtained from different model results. The horizontal axis represents both short-term (i.e. 5 years

from 1985/1995 to 2020) and long-term (i.e. 30 years from 2020 to 2080) changes (source: BMD 2016; BWDB 2016; BIWTA 2017; PSMSL 2017; UHSLC 2017 (baseline data); Table 1 (future projections))

Table 2 Projected wind directions in the coastal area of Bangladesh based on A1B trajectory. Substantial variation in the percentages of likely wind directions are projected for winter, pre-monsoon and post-monsoon seasons whereas, less variations are projected for monsoon seasons (source: IWFMM 2012)

Time-slice	Winter	Pre-monsoon	Monsoon	Post-monsoon
2020	N (21%)	SW (29%)	S (33%)	NE (19%)
2050	N (16%)	SW (23%)	S (33%)	N (14%)
2080	N (18%)	S (31%)	S (31%)	NE (12%)

moderators were applied for the same areas as used for baseline conditions. The ‘ready to run’ raster surfaces were used for scaling, weighting and generating baseline conditions and future scenarios of land susceptibility to erosion. To identify the levels of future susceptibility, the pixel values of the raster surfaces were scaled and categorised into five different susceptibility classes ranging from 1 to 5 (where 1 represents very low and 5 represents very high susceptibility). Table 3 represents the scales of the baseline susceptibility as a basis for generating future scenarios whereas, while Fig. 2 indicates the changes in percentages applied for scaling future hydro-climatic drivers. Due to data scarcity, A1B trajectory-based projections were considered as an average scenario of wind directions in the coastal area (see Table 2).

Sensitivity analysis of the LSCE model

Sensitivity analysis (SA) is the process of investigating how the variation in the model input parameters impact the outputs (Sarrazin et al. 2016). SA is essential to investigate the model behaviour by way of changing parameter values. SA is the most effective way of informing the validity of model results to decision makers (Pannell 1997). However, the performance of SA in GIS-based modelling efforts is reliant upon several decision-making processes that determine the reliability of the model outputs (Crosetto and Tarantola 2001). A GIS-based model requires a variety of spatial data that may produce a number of uncertainties originating from type, source, scale, collection methods and measurement errors (Crosetto et al. 2000). Hence, it was an essential task of the present study to conduct SA for the GIS-based LSCE model to justify the spatial resolution and to validate and communicate the results of the model in a more effective way. Moreover, the sensitivity tests indicate the level of accuracy of the LSCE model for both the baseline and future erosion susceptibility in the coastal area of Bangladesh. Following three different methods performed the sensitivity of the LSCE model:

changes of weights of the parameters, distribution of parameter values and a general versus regional model.

Weighting between parameters

The first SA was based on the weightings between the model parameters. In assessing overall (general) land susceptibility to erosion, the model considered the full (1) weights for the underlying physical elements whereas, the weights for the hydro-climatic forces were varied between 0 and 1 on the basis of experts’ opinions. The weights for the hydro-climatic factors were assigned as 0.84, 0.79, 0.71 and 0.65 for water discharge, mean sea level, rainfall and wind speed and direction, respectively. To investigate the potential changes in outputs under the changes in given weights of the parameters, this study derived four types of tests:

- Test 1: All the parameters having full (1) weight
- Test 2: A 10% decrease in weights for underlying physical elements and no changes in weights for hydro-climatic parameters
- Test 3: A 10% decrease in weights for underlying physical elements and a 10% increase in weights for hydro-climatic parameters
- Test 4: A 10% decrease in weights for all the parameters

The aim of the first three tests was to identify whether the given weights of the parameters are sensitive to erosion susceptibility in the LSCE model. The first test was designed to give full weight to all the parameters whereas the second and third tests were to reduce the gaps of weights between physical elements and hydro-climatic factors in the model. The fourth test aimed at identifying if any similarities in the results existed when under an equal decrease of weights for all the parameters. The conditions (i.e. tests) were applied to the model parameters and the new weights of the parameters are shown in Table 4.

Distribution of parameter values

The second set of SA was based on the changes in the distribution of class values (i.e. levels of susceptibility) of the model parameters. The overall erosion susceptibility was assessed based on the equal interval classification method in which, the values of the parameters were equally segmented into five susceptibility classes based on their ranges (i.e. highest and lowest). To assess the distributional sensitivity of the parameter values in the LSCE model, a new classification method was applied to the model. This has given new class values for each susceptibility class. The study first aimed to distribute the parameter values into five susceptibility classes by using the exponential growth of the dataset. Due to the diverse nature of location-based data, no homogeneity was found

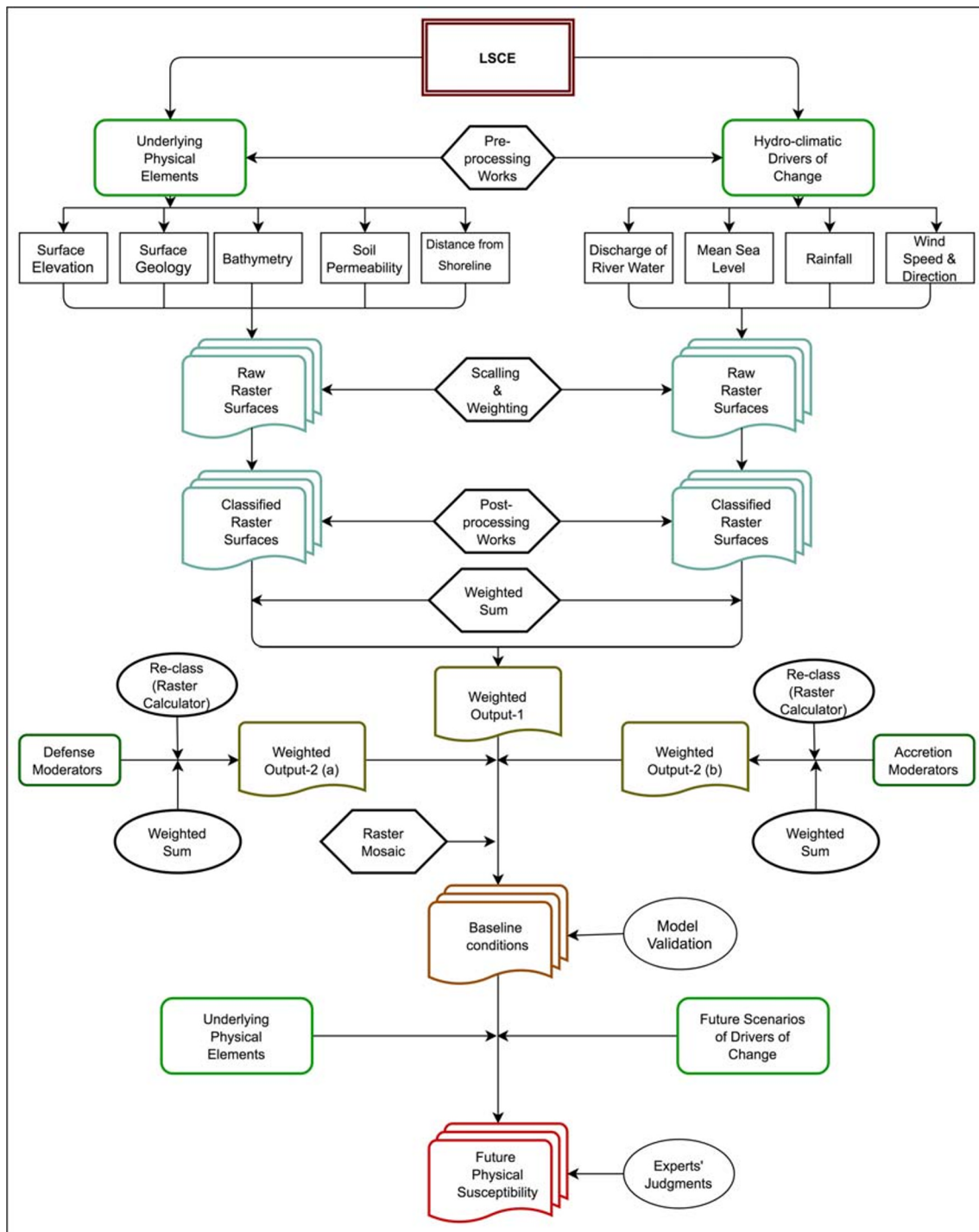


Fig. 3 A simplified schematic representation of the processes involved in the LSCE model to generate future erosion susceptibility. The pre-processing tasks included geometric, radiometric and atmospheric corrections of DEM, adjustment of vertical accuracy of DEM, making fishnet and conducting zonal statistics for bathymetric and water discharge data

whereas, post-processing works included ‘rescale by function’ and ‘fill’ operations. Baseline hydro-climatic parameters were recalculated by the future scenarios and overlaid with existing physical parameters to generate future erosion susceptibility

between the data ranges for each location. It was not possible to calculate the succeeding growth rate (*r*) of the location-based data, and hence, this study did not follow an exponential way of classifying the data for the new susceptibility classes.

The study reviewed the possible classification methods in the ArcGIS environment in which, seven types of methods (i.e. geometric interval, natural breaks (Jenks), quantile, manual, defined interval, equal interval and standard deviation) are

Table 3 Scale used for classifying the baseline raster surfaces of the LSCE model

Parameter	Time period	Very low (1)	Low (2)	Moderate (3)	High (4)	Very high (5)
Surface elevation (meter)	Overall and all seasons	> 12	9–12	6–9	3–6	0–3
Geological formation (type)	Overall and all seasons	Dihing and DupiTiila formation, Girujan Clay, Bhuban formation, BokaBil formation, Tipam Sandstone	Valley alluvium and colluvium, tidal mud, marsh clay and peat, mangrove swamp, lakes	Estuarine deposits, alluvial silt and clay, Chandina alluvium	Alluvial silt, deltaic silt, tidal deltaic deposits	Newly formed ocean and riverine deposits, Tidal sand, deltaic sand, beach and sand dune, alluvial sand
Bathymetry (meter)	Overall and all seasons	< -5	(-5)(-10)	(-10)(-15)	(-15)(-20)	> -20
Soil permeability	Overall and all seasons	Very slow	Slow	Mixed	Moderate	Rapid
Distance from shoreline (meter)	Overall and all seasons	> 400	300–400	200–300	100–200	< .100
River water discharge (m ³ /s)	Overall	13–6152	6152–12,290	12,290–18,429	18,429–24,567	24,567–30,706
	Winter	4–1766	1766–3529	3529–5291	5291–7054	7054–8816
	Pre-monsoon	4–2806	2806–5608	5608–8410	8410–11,212	11,212–14,013
	Monsoon	29–13,102	13,102–26,175	26,175–39,249	39,249–52,322	52,322–65,396
	Post-monsoon	16–6868	6868–13,721	13,721–20,574	20,574–27,427	27,427–34,280
Mean sea level (millimetre)	Overall	1845–2173	2173–2500	2500–2828	2828–3155	3155–3482
	Winter	1610–1929	1929–2248	2248–2568	2568–2887	2887–3206
	Pre-monsoon	1720–2058	2058–2395	2395–2733	2733–3071	3071–3408
	Monsoon	2105–2439	2439–2774	2774–3109	3109–3444	3444–3778
	Post-monsoon	1947–2264	2264–2580	2580–2897	2897–3214	3214–3531
Rainfall (millimetre)	Overall	123–158	158–194	194–230	230–265	265–301
	Winter	10.22–11.53	11.53–12.85	12.85–14.16	14.16–15.48	15.48–16.79
	Pre-monsoon	90–109	109–128	128–147	147–167	167–186
	Monsoon	303–421	421–540	540–659	659–777	777–896
	Post-monsoon	86–104	104–122	122–140	140–158	158–176
Wind speed (m/s)	Overall	0.76–1.16	1.16–1.57	1.57–1.98	1.98–2.39	2.39–2.79
	Winter	0.52–0.81	0.81–1.12	1.12–1.40	1.40–1.69	1.69–1.99
	Pre-monsoon	1.15–1.62	1.62–2.09	2.09–2.56	2.56–3.03	3.03–3.49
	Monsoon	0.96–1.54	1.54–2.11	2.11–2.69	2.69–3.26	3.26–3.84
	Post-monsoon	0.36–0.66	0.66–0.96	0.96–1.26	1.26–1.56	1.56–1.86

available to classify raster surfaces. The geometric interval method is suitable for continuous data but makes relatively small class intervals in areas where there is a high frequency of occurrences (Environmental Systems Research Institute (ESRI) 2018), and hence, the data with high spatial variability used in this study are not suitable for this type of classification. The Jenks natural breaks classification method minimises within class variance (i.e. the sum of squared difference) but, maximises variance between the groups. Therefore, this method is not recommended for spatial analysis that uses multiple datasets of the same geographical area (e.g. different types of raster surfaces) (de Smith et al., 2018). The quantile classification method assigns an equal number of features into each class and not suitable to include outliers (more distant observations than

others) within upper or lower quantile (ESRI 2018). As a result, this method is not suitable for seasonally varied nature of data used in this study. Moreover, the defined interval method is not completely free from human bias in classifying data. However, based on the nature of spatial data used for the present study (i.e. mostly location-specific data), the standard deviation method was found as highly suitable for the present sensitivity analysis. In this classification method, the class values can be the proportions of one-half, one-third, or one-fourth standard deviations from the mean. By using this method, it is possible to distribute the location-specific values that are above and below the mean. This study followed the standard deviation (1σ) classification method to compare how the distribution of parameter values

Table 4 The assigned weights of the model parameters to perform sensitivity analysis under changing situations of weights. Due to the full (1) weight assigned for general assessment, it was not necessary to increase the weights of the underlying physical elements in the current SA. Except for the first test, the weights of the underlying physical elements for tests 2, 3 and 4 were decreased. Except for the second test, the weights of the hydro-climatic factors were changed under tests 1, 3 and 4

Model parameter	Weight			
	Test 1	Test 2	Test 3	Test 4
Surface elevation	1	0.90	0.90	0.90
Surface geology	1	0.90	0.90	0.90
Bathymetry	1	0.90	0.90	0.90
Soil permeability	1	0.90	0.90	0.90
Distance from shoreline	1	0.90	0.90	0.90
Water discharge	1	0.84	0.92	0.76
Mean sea level	1	0.79	0.87	0.71
Rainfall	1	0.71	0.78	0.64
Wind speed and direction	1	0.65	0.71	0.58

from the mean differs from the equal interval classification method that was previously conducted.

General versus regional model

The third set of SA was devoted to comparing and analysing the outputs of the general assessment with the regional model outputs applied for the three zones separately (i.e. western, central and eastern coastal zones). The regional assessment is important since the three coastal zones possess different physical and hydro-climatic characteristics. The general assessment was carried-out by averaging the parameter values and applied for the entire coastal area followed by the equal interval method. However, the regional SA classified the data based on the region-specific ranges (i.e. lowest and highest values of each parameter for each region). This was necessary since the data ranges among the selected parameters are different from each other for the three coastal zones. For instance, the surface elevation for the central and western coastal zones range from 0 to 6 m above mean sea level. However, the surface elevation of some areas in the eastern coastal zone reaches to 327 m. Similarly, the influences of hydro-climatic factors are different for the three coastal zones. Hence, the scale of the levels of susceptibility was reclassified by applying the equal interval method for the region-specific data ranges of each parameter (see Table 5).

Process of justification

Although the study considered validated baseline erosion susceptibility (Ahmed et al. 2018b), it was uncertain as to how

precisely the selected parameters of the LSCE model incorporated the future physical erosion susceptibility of the coastal area. Considering the issue, this study applied a semi-quantitative approach to justify and enhance the model outputs on future scenarios of land susceptibility to erosion. The justification was accomplished by addressing the degree of importance of individual parameters of the model on future susceptibility. To do this, a fuzzy cognitive mapping (FCM) approach was adopted to elicit experts’ judgments by using the ‘Mental Modeler’ software (Ahmed et al. 2018c). The experts identified current and future drivers of erosion susceptibility in the coastal area and rated the relationships between the identified drivers in two separate workshops. The final ranking of the identified drivers was based on the obtained centrality scores (i.e. the sum of in-degree and out-degree). To comprehend uncertainties, the experts were also asked to rate the levels of confidence for the established relationships between the drivers in a seven point rating scale where 1 represents very low and 7 represents very high confidence.

Results

Overall future land susceptibility to erosion

The results indicate substantial changes in future scenarios of land erosion susceptibility in the coastal area compared to current baseline conditions (Fig. 4). As expected, the outputs of RCP4.5 scenario are quite similar to the results obtained for the A1B scenario. The outputs of both RCP2.6 and RCP8.5 scenarios substantially differ from A1B and RCP4.5 scenarios. The A1B and RCP4.5 scenarios modelled moderate changes for future time-slices but RCP2.6 identified less changes and RCP8.5 showed substantial changes in the amount of lands highly susceptible to erosion in the future. For instance, RCP2.6 modelled only 0.02%, 0.17% and 0.35% of lands as having a very high susceptibility to erosion for 2020, 2050 and 2080 time-slices, respectively. In contrast, RCP8.5 modelled 0.13%, 1.25% and 2.23% of very high susceptible lands for the same time-slices, respectively. In summary, all the four scenarios designate that the amount of very low susceptible lands would be reduced substantially for different time-slices that would turn more lands into high susceptibility further into the future.

Spatially, about 98.41% of the lands in the western coastal zone were identified as very low and low susceptibility to erosion for baseline conditions (see Fig. 5). The Kuakata and Rangabali areas in the exposed western zone showed moderate to high susceptibility to erosion. The future scenario of these areas, however, would be almost similar to baseline conditions in the near future (2020) (see Fig. 6). By 2050, the level of erosion susceptibility at Kuakata and some small islands in the western coastal area would be significantly

Table 5 The scale applied for the SA to analyse regional land susceptibility to erosion in the coastal area. Based on the regional ranges of the parameters, the values were reclassified into five susceptibility classes by following the equal interval method of

classification. However, the scales of the categorical values (i.e. surface geology, soil permeability and wind direction) were redistributed to the five susceptibility classes following the literature and experts' suggestions previously used for the general assessment

Model parameter	Coastal zone	Susceptibility category				
		Very low (1)	Low (2)	Moderate (3)	High (4)	Very high (5)
Surface elevation (m)	Western	> 4	3–4	2–3	1–2	0–1
	Central	> 2	1.5–2	1–1.5	0.5–1	0–0.5
	Eastern	> 16	12–16	8–12	4–8	0–4
Surface geology (type)	Western	BokaBil formation	Chandina alluvium, mangrove swamp deposits, lakes	Alluvial silt and clay	Tidal deltaic deposits	Beach and sand dune, alluvial sand
	Central	Valley alluvium and colluvium	Tidal mud, estuarine deposits, marsh clay and peat	Alluvial silt, deltaic silt	Tidal sand, deltaic sand	Newly formed ocean and riverine deposits, beach and sand dune, alluvial sand
	Eastern	Dihing and DupiTiila formation, Girujan clay, Bhuban formation	Tipam sandstone	Tidal deltaic deposits	Beach and sand dune, alluvial sand	Beach and sand dune, alluvial sand
Bathymetry (m)	Western	> - 7	(- 5)–(- 7)	(- 3)–(- 5)	(- 1)–(- 3)	< - 1
	Central	> - 16	(- 12)–(- 16)	(- 8)–(- 12)	(- 4)–(- 8)	< - 4
	Eastern	> - 6	(- 4.5)–(- 6)	(- 3)–(- 4.5)	(- 1.5)–(- 3)	< - 1.5
Soil permeability (class)	Western	Very slow	Slow	Mixed	Moderate	Rapid
	Central	Very slow	Slow	Mixed	Moderate	Rapid
	Eastern	Very slow	Slow	Mixed	Moderate	Rapid
Distance from the shoreline (m)	Western	> 800	600–800	400–600	200–400	< 200
	Central	> 400	300–400	200–300	100–200	< 100
	Eastern	> 400	300–400	200–300	100–200	< 100
River water discharge (m ³ /s)	Western	13–252	252–491	491–730	730–969	969–1207
	Central	4543–9776	9776–15,009	15,009–20,242	20,242–25,475	25,475–30,706
	Eastern	25–36	36–47	47–58	58–69	69–79
Mean sea level (m)	Western	1.84–1.94	1.94–2.03	2.03–2.13	2.13–2.22	2.22–2.32
	Central	2.21–2.36	2.36–2.51	2.51–2.67	2.67–2.82	2.82–2.97
	Eastern	2.16–2.43	2.43–2.69	2.69–2.96	2.96–3.23	3.23–3.50
Rainfall (mm)	Western	123–140	140–157	157–173	173–190	190–207
	Central	145–166	166–186	186–207	207–227	227–248
	Eastern	216–233	233–250	250–267	267–284	284–301
Wind speed (m/s)	Western	1.0–1.25	1.25–1.5	1.5–1.75	1.75–2	2–2.25
	Central	0.76–0.96	0.96–1.16	1.16–1.36	1.36–1.56	1.56–1.76
	Eastern	1.18–1.60	1.60–2.02	2.02–2.47	2.47–2.87	2.87–3.29

higher than in previous times (see Figs. 4 and 7). These areas would turn into high and very high susceptibility to erosion by 2080 (see Fig. 8).

The baseline conditions identified about 90.87% of the lands in the eastern coastal zone as very low and low susceptibility to erosion. However, an additional 3.54 km² of existing very low and low erosion susceptible lands at Moheshkhali, Kutubdia and St. Martine islands in the eastern coastal zone (see Fig. 4) would be turned into moderate to high erosion susceptible by 2020. Noticeably, a substantial amount of lands

at Chittagong, Cox's Bazar and Noakhali in the exposed eastern coastal zone (see Fig. 4) would be turned into high susceptibility to erosion by 2050 (see Fig. 7). By 2080, high erosion susceptible lands of these areas would be turned into very high erosion susceptibility.

The central coastal zone was identified as the most diversified zone of susceptibility for baseline conditions as well as for future scenarios. Along with low and moderate erosion susceptibility, some interior coastal areas in the Meghna estuary, newly accreted small islands and banks of the large

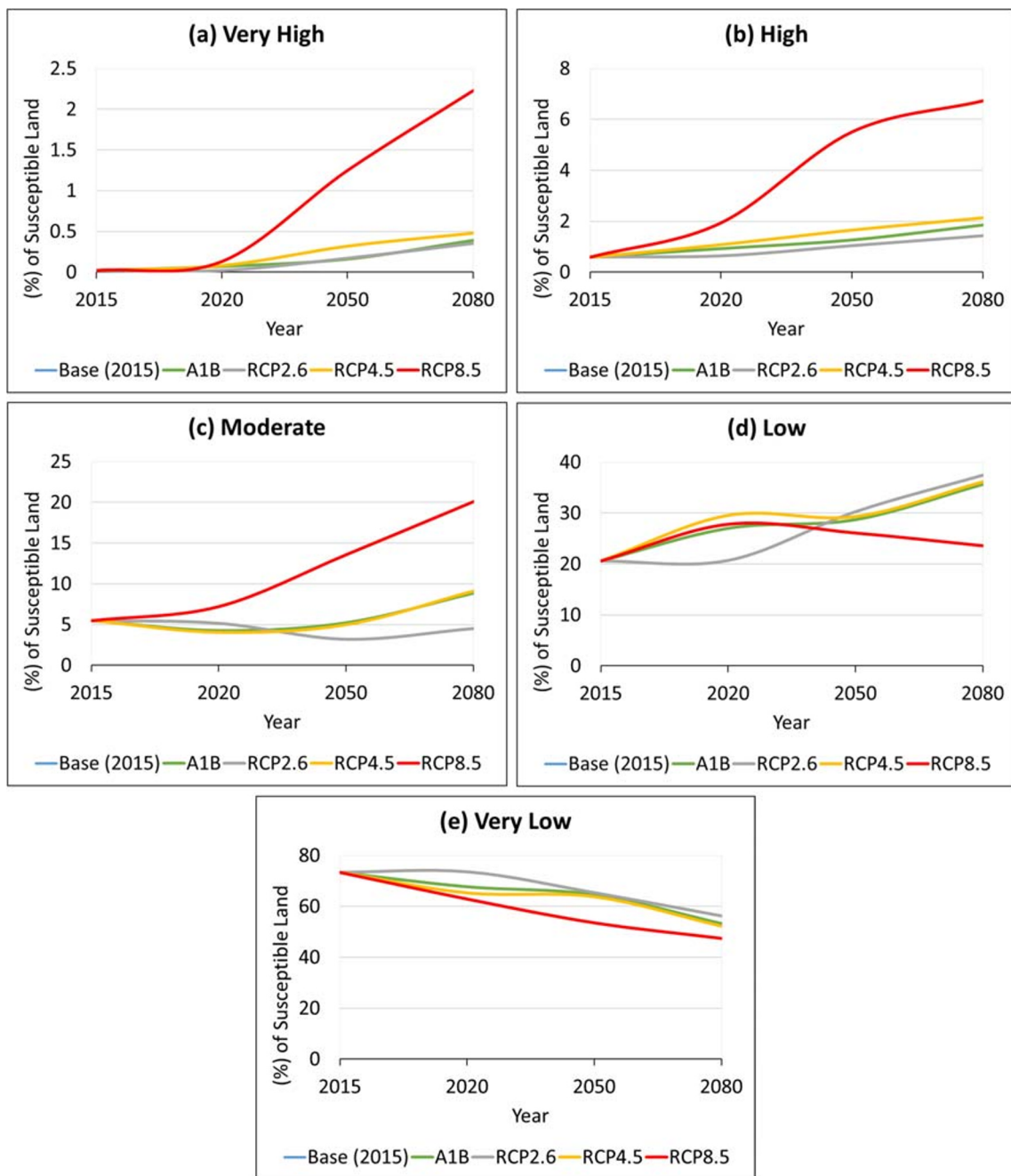


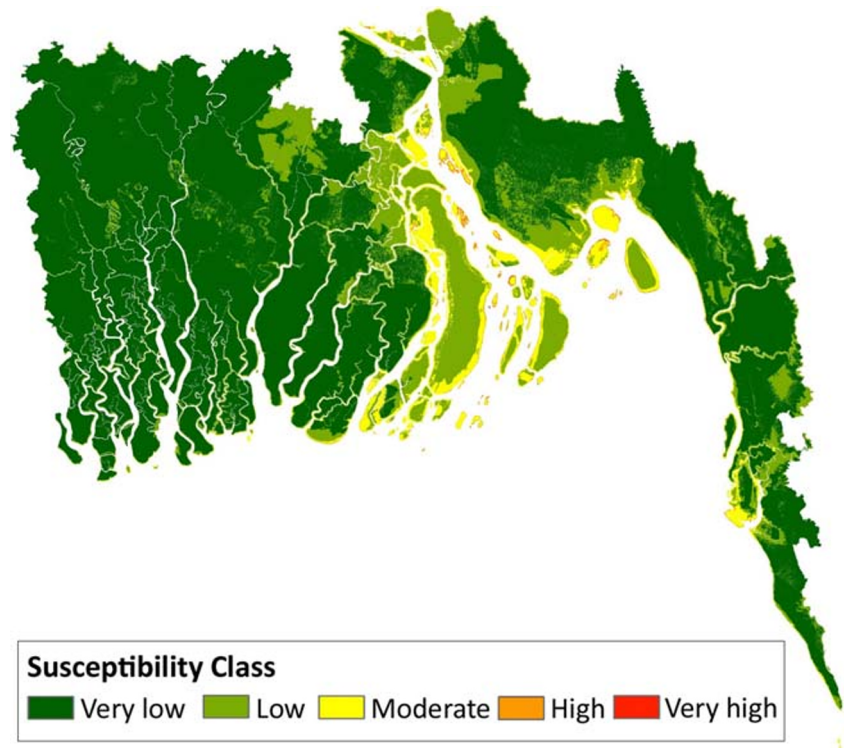
Fig. 4 Percent changes for future land susceptibility to erosion in the coastal area identified by the model under four climate trajectories for three time-slices (vertical scales are different due to varied data ranges). The total amount of 276.33 km² (0.61% of land) existing high and very

high susceptible lands would be substantially increased to 1019.13 km² (2.25% of land), 799.16 km² (1.77% of land), 1181.38 km² (2.61% of land) and 4040.71 km² (8.96% of land) by 2080 under the A1B, RCP2.6, RCP4.5 and RCP8.5 scenarios, respectively

islands in the exposed coastal areas of the central zone were identified as highly susceptible to erosion as well. These areas would be almost similar to baseline conditions by 2020 but would be turned into highly susceptible area to erosion by 2050. For instance, all of the four scenarios for 2020 time-slice identified inland areas of Noakhali, north of Monpura, Char Jonak, Bodnar Char, Dhal Char and some unnamed small islands in this zone (see Fig. 1 and Fig. 6) as being

highly susceptible to erosion. The RCP4.5 and RCP8.5 scenarios show that the lands attached to the shoreline and comparatively large islands in the central zone such as Bhola, Hatiya, Sandwip, Char Zahiruddin and Char Gazaria would be highly susceptible to erosion by 2020 (see Fig. 9). A considerable amount of currently moderate susceptible lands at Urir Char, Jahajir Char and Char Piya in the central coastal zone (Fig. 1) would also be turned into highly susceptible to erosion by the

Fig. 5 Overall land susceptibility of the coastal area to erosion for baseline (2015) conditions (Ahmed et al. 2018b). The LSCE model shows the outputs in the raster map where each pixel represents a unique level of susceptibility among the five classes of erosion susceptibility



same time. However, these inland and offshore island areas would be more susceptible to erosion under RCP8.5 scenario by 2050 than previous times (Fig. 7). The areas close to upper Meghna river (e.g. Chandpur) and the central estuarine areas (e.g. Haiderganj) (Fig. 1 and Fig. 7) would be turned into very high susceptibility to erosion by that time. By 2080, the erosion susceptibility of the mentioned areas in this zone would be higher than the scenario generated for 2050. However, most of the existing very low and low susceptible inland areas in this zone would be turned into moderately susceptible to erosion under RCP8.5 scenario by 2080 (Fig. 8).

Seasonal variation

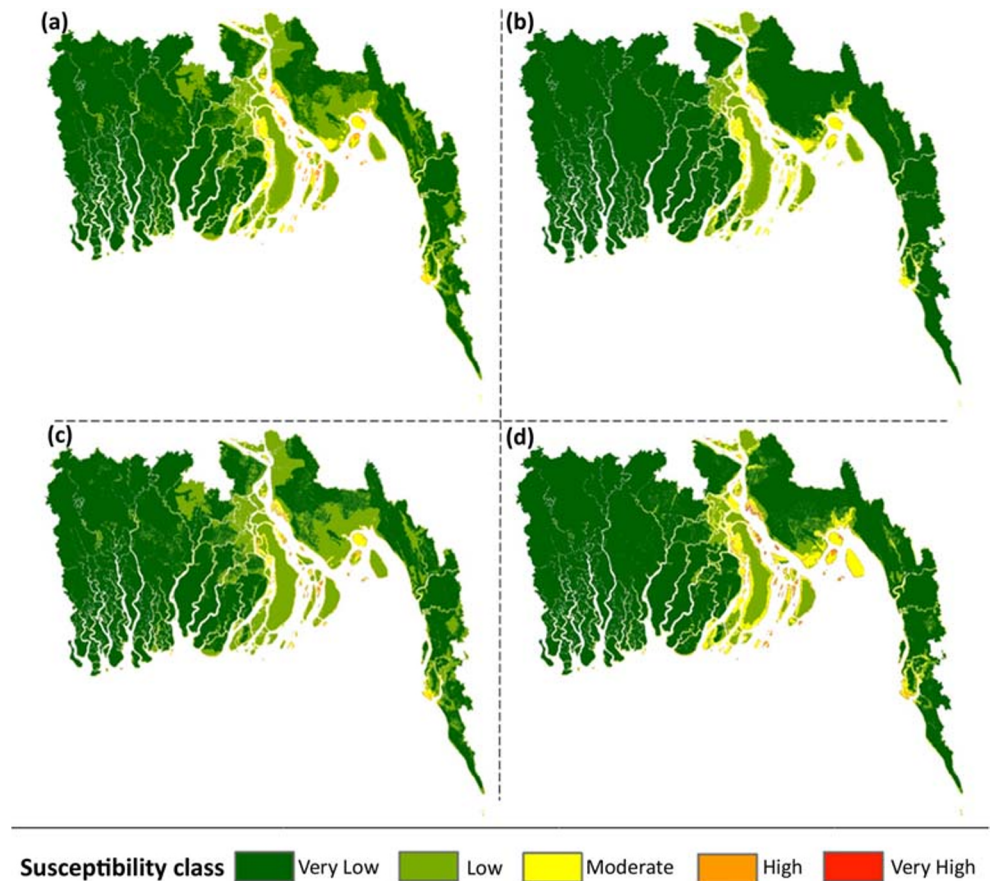
The A1B model scenario for different seasons indicates substantial amounts of spatial and temporal variations of land susceptibility to erosion in the area (Fig. 10). The results infer that winter would be the least susceptible and monsoon would be the highest susceptible season to erosion for all the time-slices. For instance, a total 14.39 km² of lands would be very highly susceptible to erosion by 2080 during winter whereas, this amount would be as high as 501.72 km² during monsoons by the same times (Fig. 10). The post-monsoon would be more susceptible to erosion than winter and pre-monsoon would be less susceptible to erosion than monsoon season. The increases of high and very high susceptible lands during future time-slices for all the seasons would consequently reduce the amounts of very low susceptible lands from baseline

conditions. Moreover, these changes would make a 3.36% increase of moderate susceptible lands further into the future (2080).

The season-based model scenario designates spatial variation of erosion susceptibility in the three coastal zones. The very low and low erosion susceptible interior areas (i.e. 98.41%) in the western coastal zone would also be quite similar for future time-slices. However, there are exceptions for Kuakata and southern Barguna areas (Fig. 1). By 2020, these areas would be altered into moderate to high susceptibility during pre-monsoon and monsoon seasons (see Fig. 10). Moreover, the low susceptible areas of the Sundarbans would be moderately susceptible during pre-monsoon but, the area would be turned into highly susceptible during monsoon season by 2050.

By 2080, the scenario of these areas would be as very high susceptibility to erosion during pre-monsoon and monsoon seasons. About 96.32% of the entire eastern coastal zone during winter and pre-monsoon seasons currently belong to very low and low erosion susceptibility (Fig. 10). However, areas of Moheshkhali and Kutubdia islands (Fig. 1) were mostly identified as moderate and high susceptibility to erosion for all of the seasons under baseline conditions. Additionally, areas such as Bhatiari and Kumira (Fig. 1) were also identified as highly susceptible to erosion. By 2080, the scenario of these areas would be turned into high and very high susceptibility during pre-monsoon and monsoon seasons. Similarly, the areal extent of moderate susceptible lands would be increased in this coastal zone during pre-monsoon seasons by the same times. Moreover, the exposed part of this zone having very

Fig. 6 Susceptibility of the coastal area to erosion by 2020 for **a** A1B, **b** RCP2.6, **c** RCP4.5 and **d** RCP8.5 scenarios. The susceptibility maps indicate that the variation in land susceptibility under A1B and RCP4.5 are less. On the other hand, the variation in the levels of susceptibility under RCP2.6 and RCP8.5 are clearly reflected in the maps



low susceptibility would turn into low to moderate susceptibility during post-monsoon seasons by 2080 (Fig. 10).

The central coastal zone, however, currently resembles sizeable amounts of moderate, high and very high erosion susceptible lands for all the seasons (vary from 2.2% during pre-monsoon to 7.81% during post-monsoon in total). The amounts of high and very high susceptible lands were 138.59 km² and 624.27 km² during pre-monsoon and monsoon seasons in this zone compared to 83.53 km² and 246.22 km² during winter and post-monsoon seasons, respectively. By 2080, the areal extent of these lands would be comparatively higher than the baseline for all of the seasons. For instance, the shoreline and associated inland areas at Haiderganj, Rahamat Khali of Laksmipur district, Nazirpur and some islands such as Char Lakkhi, Char Kashem, Andher Char of Patuakhali district, Dhal Char, Char Nizam, Char Kukri-mukri, Sona Char and Monpura of Bhola district (Fig. 1) would be high and very high susceptibility to erosion during monsoon season by that time (Fig. 10). However, some islands such as Urir Char, Char Pial, Char Hasan in this zone would be turned from low to moderate susceptibility during winter seasons by 2080 (Fig. 10).

Some islands namely, Sandwip, Monpura and Jahajir Char currently belong to moderate to high and very high erosion susceptibility during post-monsoon seasons but, the situations

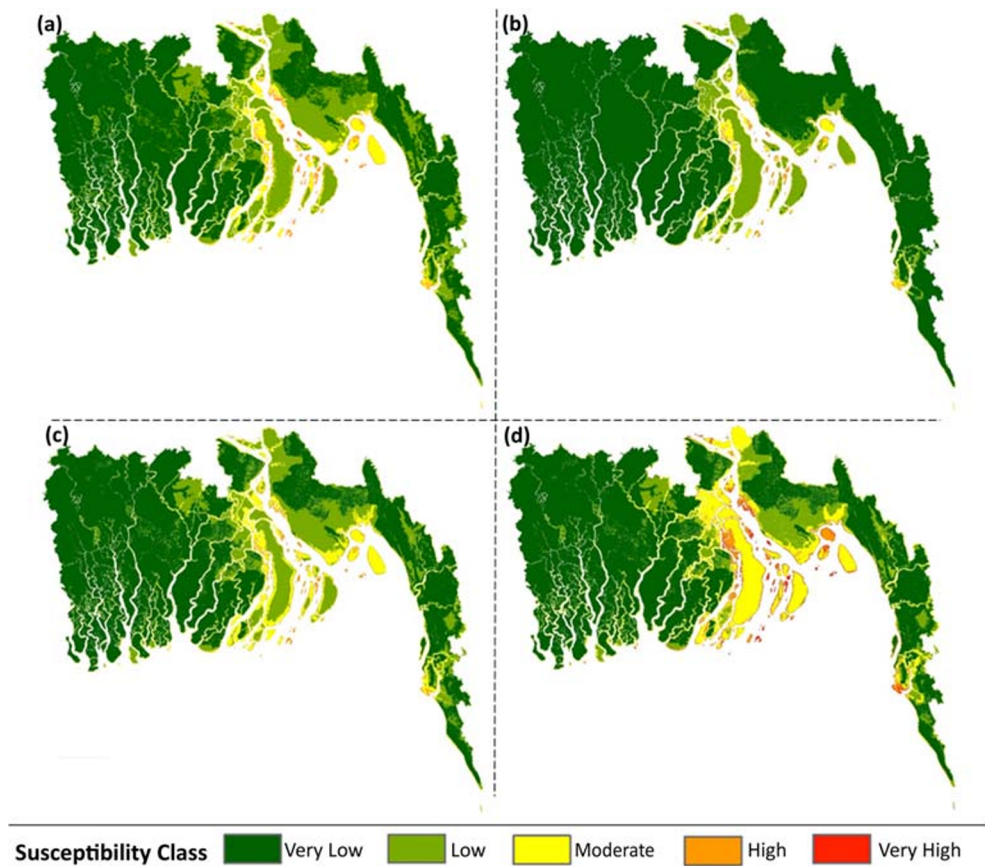
of these areas would be severe during monsoon and post-monsoon seasons by 2080 (Fig. 1 and Fig. 10). On the other hand, the interior areas of this zone would be varied spatially for all the seasons by 2050 but, would be turned into moderate and high erosion susceptibility during pre-monsoon and monsoon seasons by 2080.

Discussion

Sensitivity and accuracy of the model

The SA by way of changing the weights of the model parameters indicates small changes for the first and second tests and considerable changes for the third test compared to the general assessment (see Fig. 11). As expected, the fourth test resulted in no changes in the levels of susceptibility to erosion. The probable reason behind the slight change in the levels of susceptibility under test 1 could be due to the impacts of hydro-climatic factors (i.e. increases of 10% weights). The assignment of full (1) weights for the hydro-climatic factors made 13.44%, 16.59%, 20.59% and 22.75% increases of weights in the model for water discharge, mean sea level, rainfall and wind speed and directions, respectively, from the previously assigned weights of 0.84, 0.79, 0.71 and 0.65 for the same

Fig. 7 Susceptibility of the coastal area to erosion by 2050 for (a) A1B; (b) RCP2.6; (c) RCP4.5 and (d) RCP8.5 scenarios. The likely changes in the levels of land susceptibility to erosion are highly discernible by 2080 under the RCP8.5 scenario



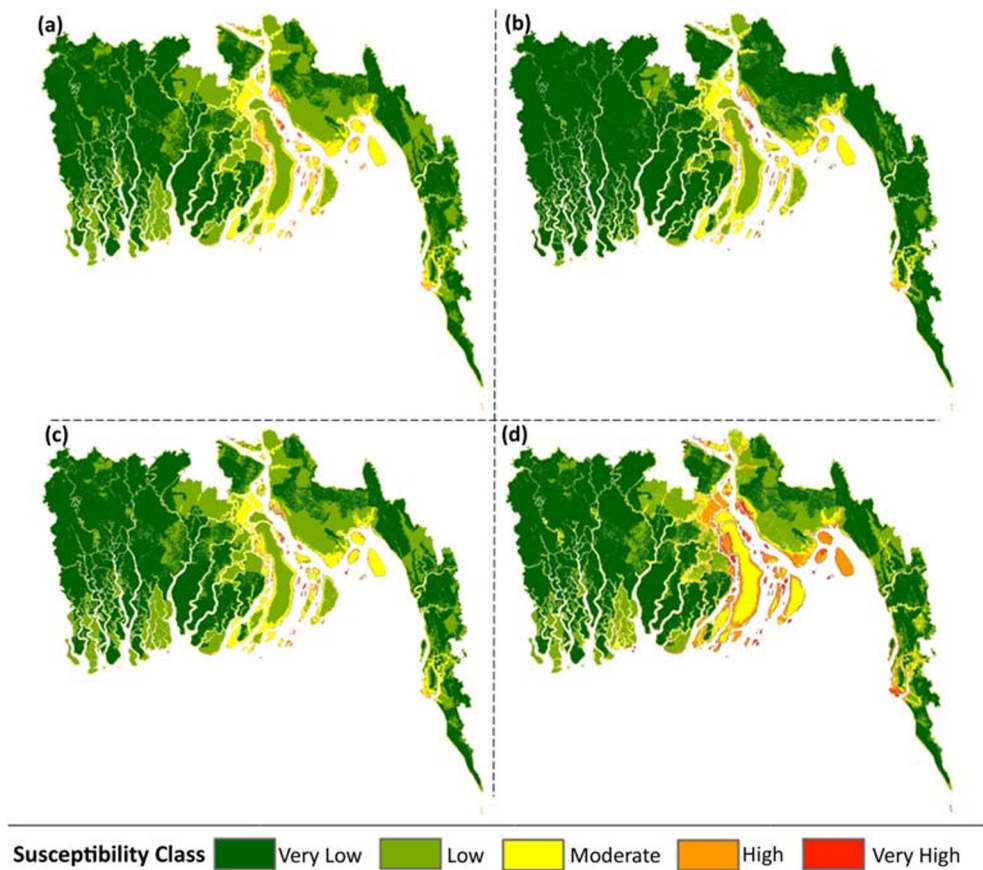
parameters by the experts. Since there is a substantial influence of hydro-climatic factors in the central coastal zone, the changes were reflected in the offshore islands and newly accreted coastal lands (Ahmed et al. 2018b). The probable controls of underlying physical conditions on erosion susceptibility were visible under the second test of weighting in which a 10% decrease in the underlying physical elements resulted in almost similar kind of changes in the levels of erosion susceptibility as obtained for the first test.

The impacts of hydro-climatic factors were highly visible for the third test under the situation of a 10% decrease in weights for underlying physical elements and a 10% increase for hydro-climatic parameters. However, the SA produced no changes in the level of susceptibility under the fourth test. This similar result with the general assessment indicates that the weightings of the parameters in the LSCE model are sensitive. The current sensitivity analysis by changing 10% weights indicates that both the underlying physical conditions and hydro-climatic factors are sensitive for the model but, very less changes were observed for the SA in comparison with the general assessment. The present study assumes that further variations in the weights of the parameters (e.g. 15%, 20% and so on) might change the levels of erosion susceptibility in the LSCE model.

The SA by way of redistributing the parameter values into five susceptibility classes indicates less substantial changes in the levels of land susceptibility to erosion for baseline condition (Table 6). The assessment infers that redistributing the ranges of susceptibility classes are not substantially sensitive for the present study area. The probable reason behind these minor changes might be due to several possible reasons. Firstly, the parameter values for surface geology and soil permeability were similar to the general assessment. Secondly, the data ranges of susceptibility classes for underlying physical elements were reduced under this new classification method but, these changes in the data ranges were balanced by the increases of data ranges for the susceptibility classes of hydro-climatic factors. However, the redistribution of the distances from the shoreline is thought to be an influential reason for minor changes observed in the assessment.

The regional (i.e. coastal zones) SA shows the probable impacts of the varied nature of underlying physical elements and hydro-climatic factors in the area more precisely than the other two methods. For instance, due to the probable impacts of hydro-climatic factors along with low surface elevations and low bathymetric depths in the exposed central coastal zone, the regional model identified comparatively more high and very high susceptible lands in the central coastal zone than the western and eastern zones (Table 7). The lowest average

Fig. 8 Susceptibility of the coastal area to erosion by 2080 for **a** A1B, **b** RCP2.6, **c** RCP4.5 and **d** RCP8.5 scenarios. Although the changes in the levels of land susceptibility to erosion show substantial variations among the four scenarios, major changes are projected under the RCP8.5 scenario



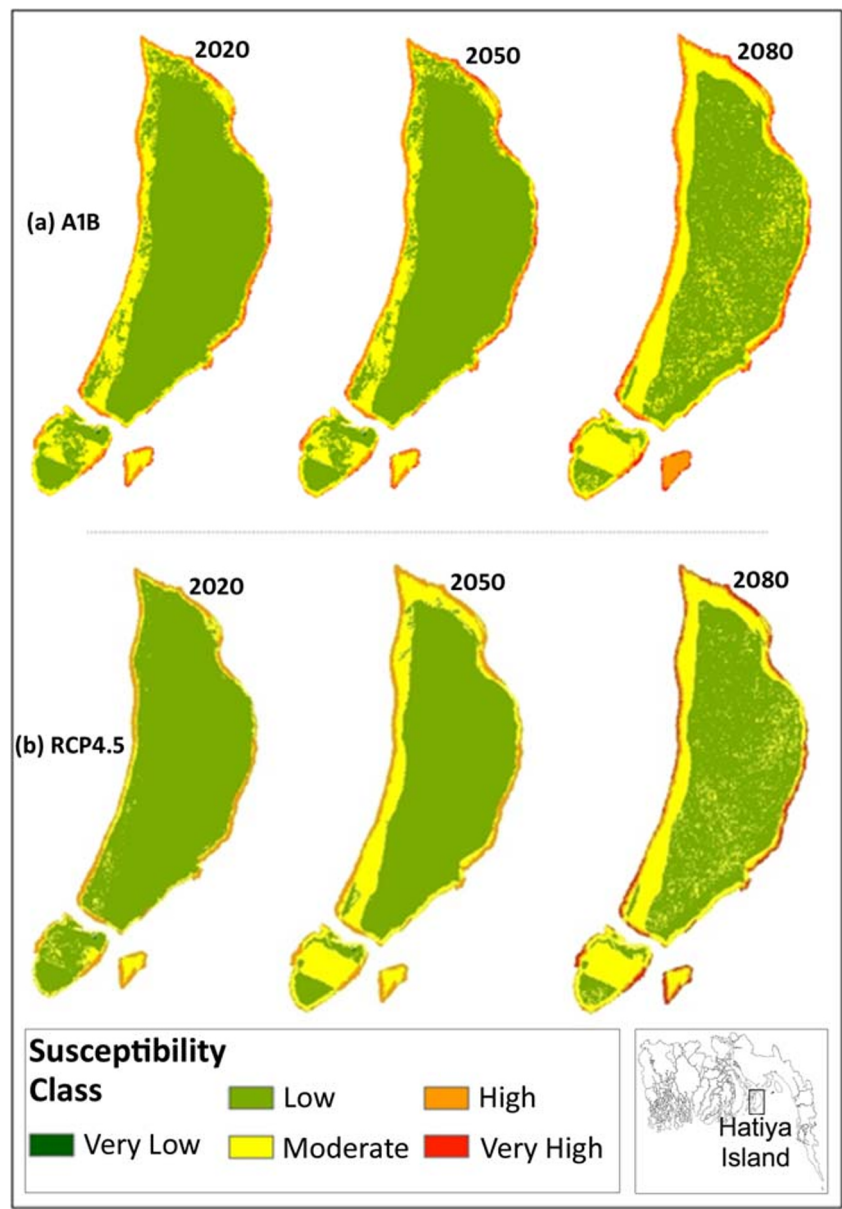
water discharge of 13.70 m³/s for the Dakatia and 25.70 m³/s for the Bogkhali river in the western and eastern coastal zones respectively during winter season were much lower than the lowest discharge (i.e. 4543.15 m³/s) recorded for the Meghna river in the central coastal zone (BWDB, 2016). During monsoon season, this lowest discharge in the central coastal zone amounted to 31,120.14 m³/s. Moreover, the lowest average mean sea level in the central coastal zone for the years from 1986 to 2015 was recorded as 2.21 m at Char Chenga, that was higher than the western (i.e. 1.85 m at Hiron Point) and eastern (i.e. 2.16 at Cox’s Bazar) coastal zones (BIWTA 2017; PSMSL 2017; UHSLC 2017).

The highest average mean sea level in the central coastal zone for the same time-period was also higher (i.e. 2.97 m at Sandwip) than the western coastal zone (i.e. 2.32 m at Khepupara) but, less than the eastern coastal zone (i.e. 3.48 m at Chittagong). Moreover, the amount of annual average rainfall in the central coastal area was higher (i.e. lowest 145.68 mm at Chandpur and highest 247.97 mm at Sandwip) than the western coastal zone (i.e. lowest 123.36 mm at Jessore and highest 206.5 mm at Khepupara) (BMD, 2016). However, the amount of rainfall in the central coastal zone was lower than the eastern coastal zone (i.e. lowest 216.84 mm at Chittagong and highest 301.4 mm at Teknaf).

The impacts of low surface elevation and bathymetric depths on the levels of erosion susceptibility for the western and eastern zones were reflected in the sensitivity analysis. Comparatively low water discharges, low mean sea level and less amount of rainfall in the western coastal zone were the probable reasons for less changes in the levels of erosion susceptibility compared to the central coastal zone. Further, the probable impacts of hydro-climatic factors were compensated for by the favourable types of surface geology and low permeability of soils in the eastern coastal zone under this regional sensitivity analysis.

The three types of sensitivity analysis in the present study infer that the model parameters are less sensitive in respect of weightings (except the third test) and redistribution of parameter values but, considerably sensitive for regional analysis (especially for the central coastal zone). Moreover, the applicability of the LSCE model needs to consider carefully the assignment of weights for the parameters. One way of assessing parameter weights might be by relying upon the experts’ comments that the current study followed for the general assessment. Distribution of parameter values for the susceptibility classes might be important for seasonal analysis in which variation in the data range is large but not substantial for the general assessment that the present SA indicates.

Fig. 9 An example of likely changes in the levels of erosion susceptibility of an offshore island (i.e. Hatiya) located in the central coastal zone under the **a** A1B and **b** RCP4.5 scenarios. The current amount of 0.87 km² very high susceptible lands of the island would be increased to 1.53 km², 5.32 km² and 8.42 km² under A1B scenario for 2020, 2050 and 2080 time-slices respectively. The RCP4.5 scenario shows the likely increases of 1.04 km², 4.67 km² and 7.23 km² lands for the same time-slices, respectively. The similar amounts of changes under the scenarios indicate the strong possibility of such changes in future land susceptibility to erosion of the island



However, the regional or site-specific parameters need to be considered as the most important factors of erosion susceptibility for the coastal area in a situation where the physical settings and hydro-dynamic conditions vary considerably (e.g. central coastal zone of the country).

Justification of the results

The panel of experts in the workshops identified, ranked and mapped 33 relevant components for baseline conditions and for near future (2020), 36 components for future (2050) and 42 components for far future (2080) that include both physical and human aspects of land susceptibility to erosion in the coastal area (Ahmed et al., 2018c). This study recognised the nine drivers used in the LSCE model that were identified

as having higher centrality scores than other components in the FCMs by the panel of experts under three time-slices (Table 8). The model outputs were also evaluated in the discussion segments of the workshops. Furthermore, the confidence ratings obtained from the workshops postulate that the ratings for sea level rise, water discharge, soil permeability and defence structures were assigned by the experts with high to very high confidence. The workshops rated the issues of accretion (sedimentation) with moderately high confidence, whereas the issue of wave actions was rated with moderately low confidence. The FCM-based high-scored components and their confidence ratings correspond with the model parameters and their given weights (Table 8), which fairly justify the inclusion of the model parameters and their influences on future scenarios of erosion susceptibility in the area.

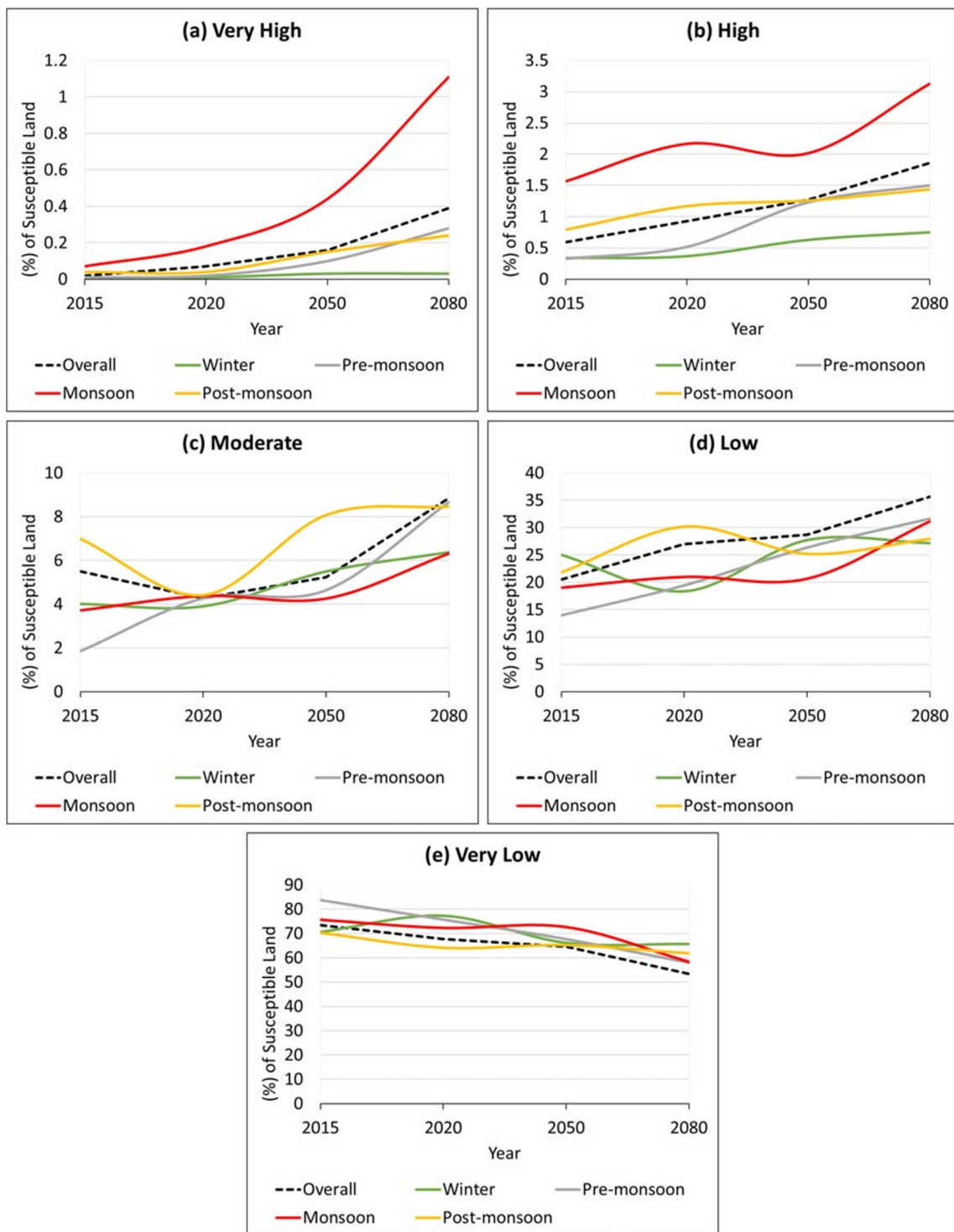


Fig. 10 The seasonal variation of the percentages of susceptible land changes for **a** very high, **b** high, **c** moderate, **d** low and **e** very low susceptibility categories under the A1B scenario in comparison with the overall baseline conditions for the three time-slices. The figure shows that

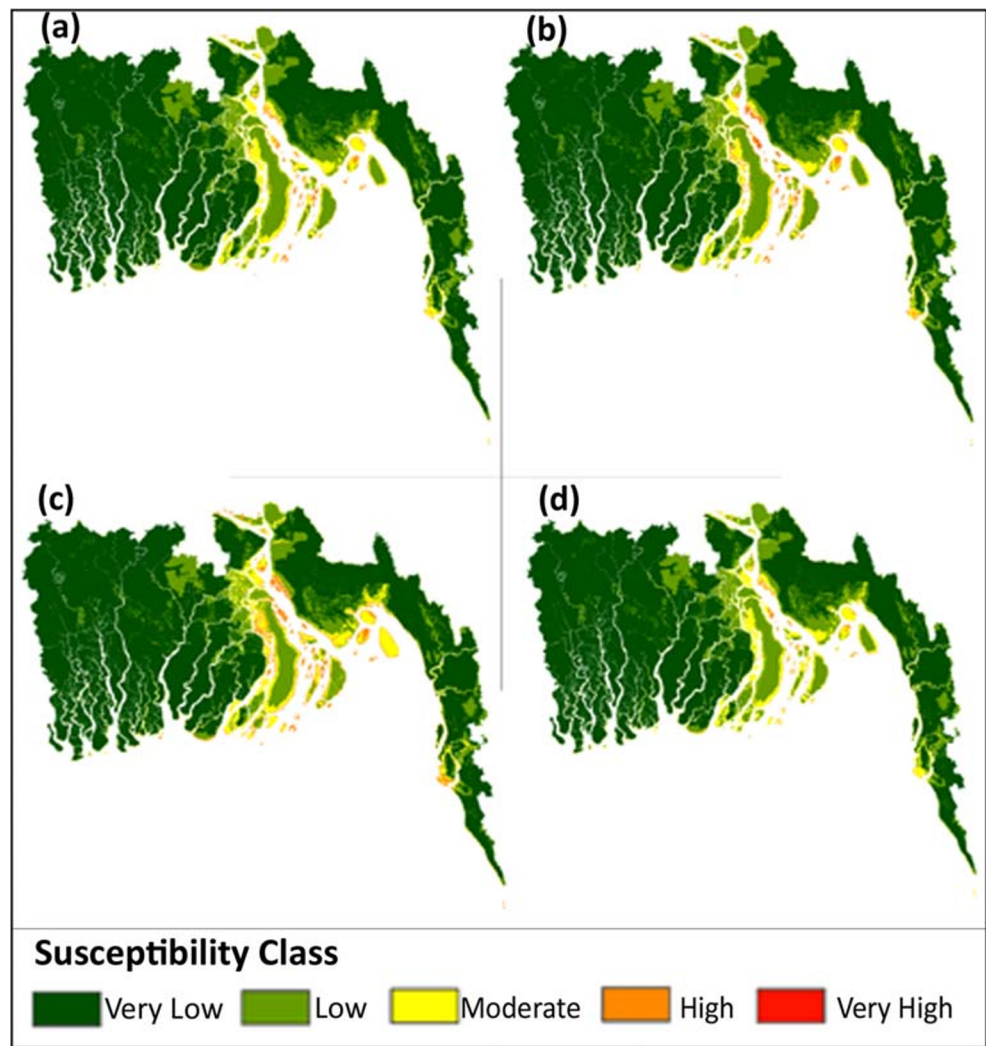
the percentages of susceptible lands for very high and high susceptibility classes are varied from the baseline for monsoon season compared to pre-monsoon, post-monsoon and winter seasons

Influence of hydro-climatic drivers

The impacts of the predicted changes in hydro-climatic triggering factors (Fig. 2) would be substantial for future

land susceptibility to erosion (Fig. 4) in the coastal area. This study suggests water discharge and rainfall as key drivers of future susceptibility to erosion in the area. Except for RCP2.6, all other scenarios show a considerable

Fig. 11 The spatial variation of the results identified for the four sorts of weightings of the model parameters: **a** test 1, **b** test 2, **c** test 3 and **d** test 4. The maps indicate a minor amount of changes in the susceptibility classes for the western and eastern coastal zones. However, noticeable changes were identified for the central coastal zone under the third sort of SA test (map c)



increase of future water discharge of the coastal rivers in the area. For instance, the A1B and RCP4.5 climate scenarios show similar increases of future coastal river water discharges that would be increased as 30.7% and 27.4% respectively by 2080. This increase would be as high as 39.1% by 2080 under the RCP8.5 scenario. Along with discharge, the likely increases of future rainfall under

A1B, RCP4.5 and RCP8.5 are noteworthy. Although the amount of rainfall under RCP8.5 is projected to decrease by 2050, it would be increased to 13.76% by 2080 from the baseline. These increases in future water discharge and rainfall seem to have extensive impacts on future land susceptibility generated by the model scenarios.

Table 6 Comparison of the results obtained for general assessment and sensitivity analysis. The results indicate very similar amounts of susceptible lands for the coastal area obtained by performing the equal interval and standard deviation (1 σ) classification methods

Susceptibility class	Method of distribution			
	Equal interval (general assessment)		Standard deviation (1 σ) (sensitivity analysis)	
	Area	%	Area	%
1 (very low)	33,163.79	73.34	33,133.08	73.27
2 (low)	9296.71	20.56	9286.04	20.535
3 (moderate)	2483.70	5.49	2536.87	5.61
4 (high)	266.32	0.59	254.14	0.562
5 (very high)	10.01	0.02	10.40	0.023
Total	45,220.53	100	45,220.53	100

Table 7 Comparison of area and percentages between general (overall) and regional model of land susceptibility to erosion. The combined results for the three zones show that the major changes occurred for very high and high susceptibility classes

Susceptibility class	Area		Percentage	
	Overall	Zone-wise	Overall	Zone-wise
1 (very low)	33,163.79	31,374.91	73.34	69.38
2 (low)	9296.71	9635.98	20.56	21.31
3 (moderate)	2483.70	3774.84	5.49	8.35
4 (high)	266.32	416.15	0.59	0.92
5 (very high)	10.01	18.65	0.02	0.04
Total	45,220.53	45,220.53	100	100

The future level of high erosion susceptibility might be accelerated by the likely increases of mean sea level. Model data for A1B scenario shows that there will be 0.08%, 0.24% and 0.42% increases in MSL from baseline by 2020, 2050 and 2080, respectively. In contrast, the RCP2.6 scenario shows an increasing scenario of MSL but, the increase would be comparatively lower than other scenarios. More importantly, the RCP8.5 scenario shows the highest increases of 0.31% and 0.48% MSL from baseline by 2050 and 2080, respectively. These increases of future mean sea level could inundate more coastal lands and hence, the lands would be highly affected by wave actions. Since all the climate scenarios show the likely increases in wind speeds, the probable impacts of the directions of prevailing southern and southwestern winds (IWMF,

2012) would be higher in future than present times. Notably, the RCP8.5 scenario shows an increase of 5.31% wind speed by 2080 than baseline. The increasing scenarios of future wind speeds and consequent wave actions, together with the high volume of water discharge, heavy rainfall and high mean sea level would have probable impacts on erosion susceptibility in the coastal area that would turn more lands into high erosion susceptibility in the future.

Response from physical elements

Although the impacts of the four hydro-climatic triggering factors are found to be increased in future for most of the scenarios, the underlying physical elements of the three coastal zones could react to the changes differently. For instance, the impacts of hydro-climatic triggering factors seem to be minimal in the western coastal zone compare to other zones for future time-slices and hence, the results of the LSCE model showed considerably lower erosion susceptibility in the western zone than the central and eastern zones. This result suggests probable responses from favourable surface geology and geomorphic features (i.e. valley alluvium and marsh clay and peat, mangrove swamp) and moderate soli permeability of the zone on its low erosion susceptibility. Additionally, the interior western coastal zone is not very close to the exposed coast that would make the areas free from potential impacts of wave actions and longshore currents in future. However, shallow bathymetric depths (i.e. - 5 to - 15 m) would have probable impacts on wave-induced erosions at Barguna and Patuakhali areas. Likewise, the reason behind the moderate susceptibility

Table 8 Top 10 FCM components based on centrality scores (in bracket). The corresponding parameters of the LSCE model marked as italic

Baseline (2015)	Near future (2020)	Future (2050)	Far future (2080)
Rate of sedimentation (8.9) <i>(Accretion Handicap)</i>	Wave action (9.82) <i>(Proxy: Wind speed)</i>	Rate of sedimentation (15.59) <i>(Accretion Handicap)</i>	Rate of sedimentation (20.28) <i>(Accretion Handicap)</i>
Wave action (8.81) <i>(Proxy: Wind speed)</i>	Rate of sedimentation (9.76) <i>(Accretion Handicap)</i>	Wave action (11.59) <i>(Proxy: Wind speed)</i>	Wave action (16.83) <i>(Proxy: Wind speed)</i>
Variation of tidal range (7.79)	Variation of tidal range (8.3)	Upstream sediment input (10.75)	Variation of tidal range (13.86)
Cyclone and storm surges (7.4) <i>(Proxy: Wind speed)</i>	Cyclone and storm surges (7.93) <i>(Proxy: Wind speed)</i>	Embankment (10.64) <i>(Defence handicap)</i>	Embankment (10.71) <i>(Defence handicap)</i>
Soft and unconsolidated soil (5.89) <i>(Geological formation)</i>	Soft and unconsolidated soil (6.53) <i>(Geological formation)</i>	Variation of tidal range (10.53)	Sea level rise (10.35) <i>(Mean sea level)</i>
River water discharge (5.48) <i>(River water discharge)</i>	River water discharge (5.81) <i>(River water discharge)</i>	Cyclone and storm surges (9.49) <i>(Proxy: Wind speed)</i>	River water discharge (10.33) <i>(River water discharge)</i>
Embankment (5.01) <i>(Defence handicap)</i>	Embankment (5.42) <i>(Defence handicap)</i>	Soft and unconsolidated soil (8.59) <i>(Geological formation)</i>	Rainfall (7.71) <i>(Rainfall)</i>
Rainfall (3.15) <i>(Rainfall)</i>	Rainfall (3.47) <i>(Rainfall)</i>	River water discharge (7.36) <i>(River water discharge)</i>	Bathymetry (7.06) <i>(Bathymetry)</i>
Bathymetry (2.73) <i>(Bathymetry)</i>	Bathymetry (2.93) <i>(Bathymetry)</i>	Sea level rise (7.12) <i>(Mean sea level)</i>	Monsoon wind (4.74) <i>(Proxy: Wind speed)</i>
Sea level rise (2.59) <i>(Mean sea level)</i>	Sea level rise (2.77) <i>(Mean sea level)</i>	Rainfall (6.33) <i>(Rainfall)</i>	Compaction of sediment (4.06) <i>(Soil permeability)</i>

in the eastern coastal zone is closely associated with the underlying physical elements.

It is important to note that the values of the three hydro-climatic drivers were found to be comparatively higher in this zone than other zones for current and future time-slices. However, the effects of the drivers would be less due to higher surface elevations, favourable geomorphic features and very slow permeability of soils in the zone. For instance, the probable occurrences of heavy rainfall might be increased to 403.74 mm by 2080 in the eastern coastal zone but, the potential impacts on erosion susceptibility would be minimal due to its hard and unconsolidated surface geology.

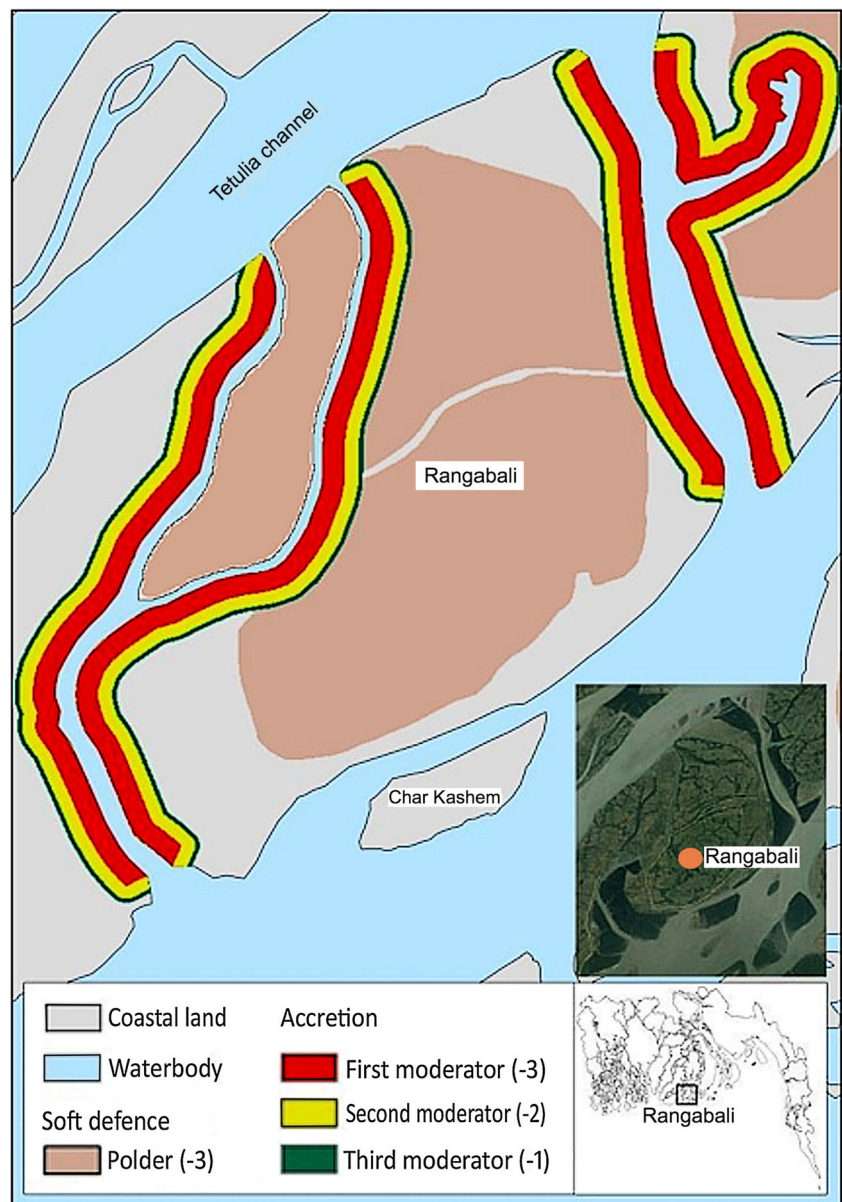
The likely impacts of heavy rainfall would be highly visible only in the islands such as Kutubdia, Moheshkhali and St. Martin of the zone where the silt and clay-dominated soils

are highly responsive to erosion. In contrast, the geomorphic features (e.g. newly formed ocean and riverine deposits, tidal sand, deltaic sand, beach and sand dune, estuarine deposits, tidal deltaic deposits, etc.), together with mixed and rapid soil permeability in the central coastal area would be highly favourable for the hydro-climatic drivers to increase erosion susceptibility in future.

Seasonal influences

The seasonal fluctuations of the hydro-climatic drivers under the A1B scenario suggest considerable influences on land susceptibility to erosion in the coastal area. The likely impacts of the drivers would be highest during monsoon and lowest during winter compared to pre-monsoon and post-monsoon

Fig. 12 An example of the uses of moderators in the LSCE model domain. The three sets of accretion moderators were used to address the impacts of accretion whereas, the moderators for defence structures were used to discourage the human interventions in the process of erosion. The map shows the use of such moderators for Rangabali area in the central coastal zone where a substantial amount of land was accreted for the years from 1985 to 2015



season. For instance, a comparatively less amount of total water discharge (i.e. 15,160.91 m³/s) would be experienced by the coastal area during winter seasons but the volume of discharge would be as high as 96,459 m³/s during monsoon seasons by 2080. These variations in water discharge would have probable impacts on future levels of erosion susceptibility in the Meghna estuary area where the bathymetric depths are high.

Similar to water discharge, the future scenario for MSL would be least (i.e. 2.35 m) during winter and highest (i.e. 4.51 m) during monsoon season by 2080 that might inundate considerable amount of lands in the central coastal zone during monsoon season. Mean sea levels in areas attached to Sandwip channel, Urir Char and Jahajir Char in the central coastal zone (Fig. 1) would be increased between 4.18 and 4.51 m during monsoon season from the baseline 1.61 and 3.44 m by 2080.

Similarly, the current highest range of 777–896 mm rainfall in the coastal area would be increased to 1040–1199 mm by 2080. This amount of rainfall would have substantial influences to increase the level of erosion susceptibility at Patuakhali and Barguna (Fig. 1) in the exposed western coastal zone.

The projected scenario of wind speeds indicates frequent occurrences of tropical cyclone and associated storm surges during pre-monsoon and post-monsoon season in the area that would trigger wave actions in areas attached to shallow water depths in future.

Impact of human interventions

The potential human interventions (i.e. building of polder, land zoning, mangrove afforestation and land reclamation

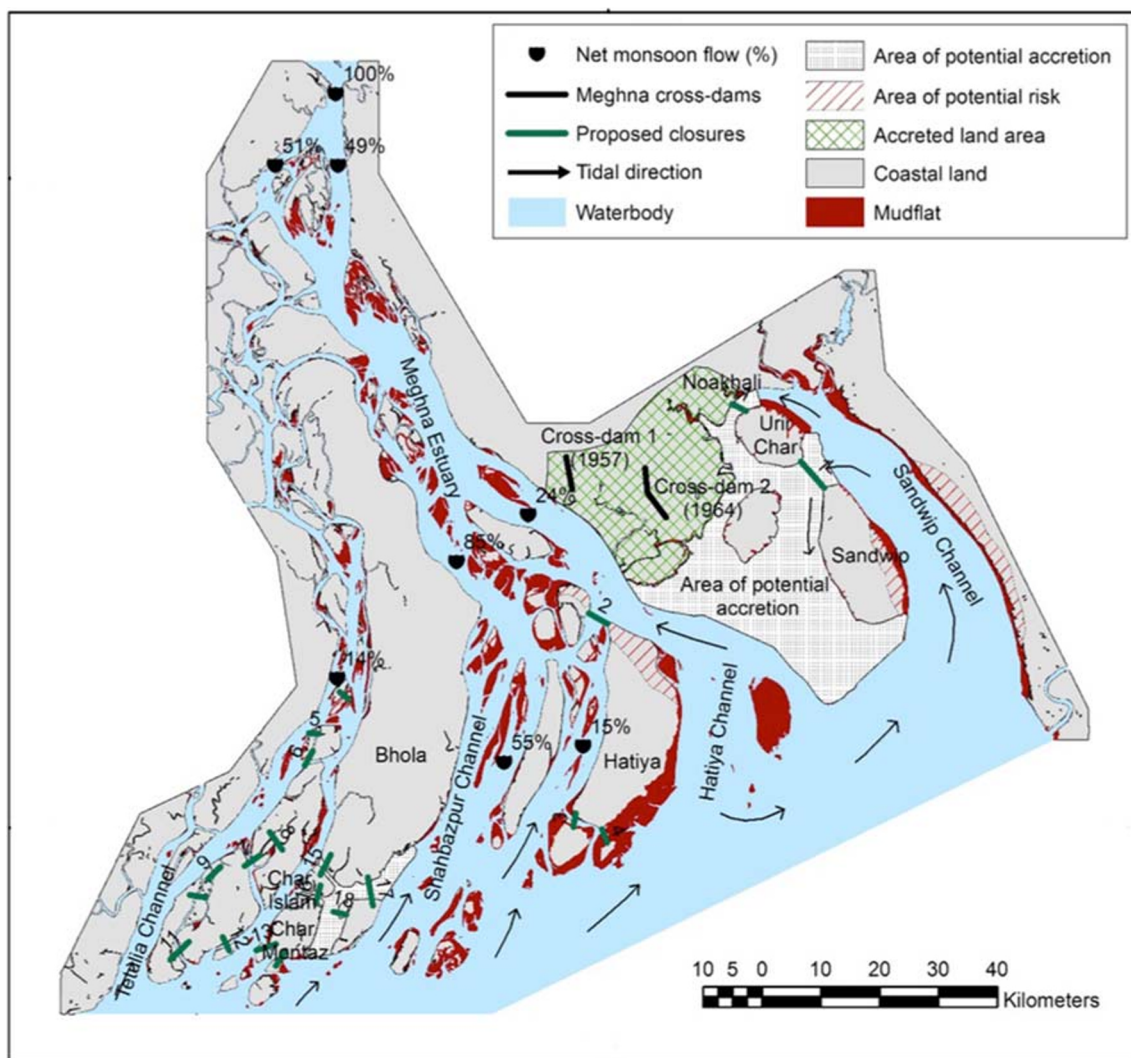


Fig. 13 Potential impacts of human intervention in the central coastal zone. The net monsoon flow in Tetulia and upper Hatiya channels are comparatively lower than the main Shahbazpur channel (Akhter and Mahmud, 2007). The net flow of southern Shahbazpur channel splits into different directions. The map shows the outcome of past land reclamation

projects as well as future predictions. Among 19 proposed closures, Sandwip-Urir Char-Noakhali and Char Montaz-Char Islam-Bhola would be highly crucial for land reclamation in the area (data source: BWDB, 2016; WARPO, 2018)

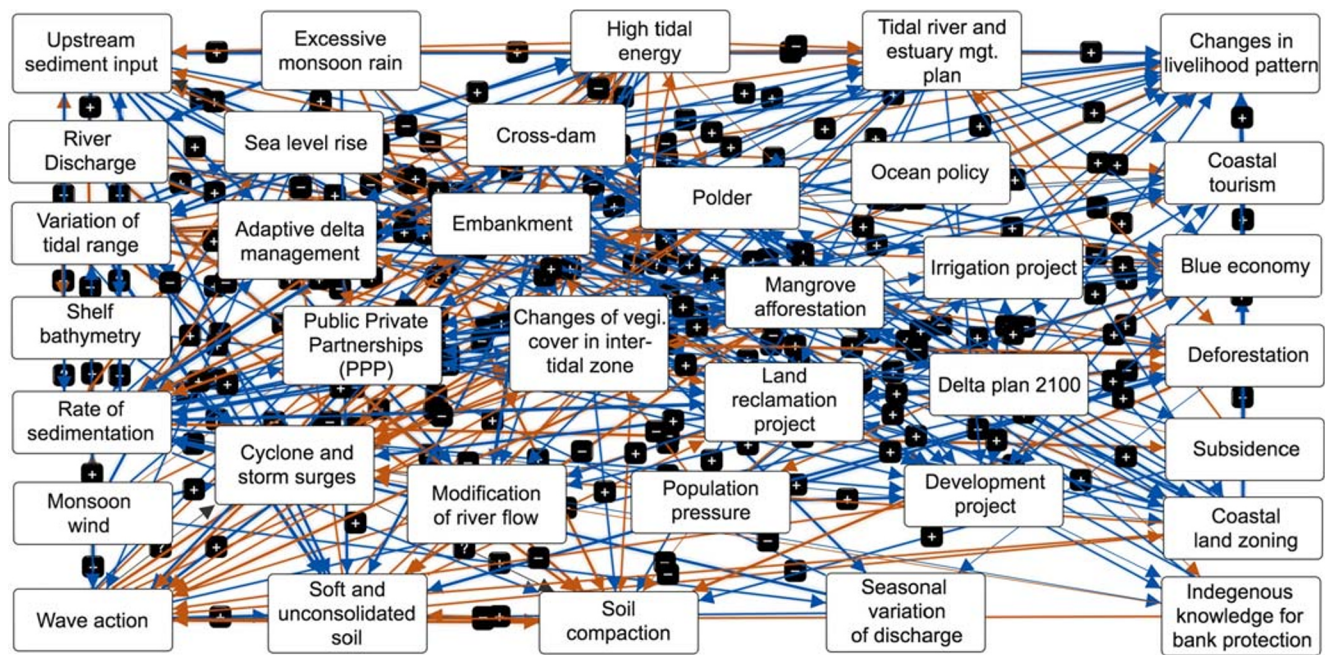


Fig. 14 Fuzzy cognitive map on potential human interventions in the coastal area in future (Ahmed et al., 2018c). The experts identified a number of human-induced factors that are important for future land

susceptibility to erosion in the area by using FCM in which the grey arrows indicate positive impacts and the grey arrows indicate negative impacts among and between the factors

project) might create an enabling condition for the government to manage highly erosion susceptible coastal lands in the area in future. Government intervention in managing coastal erosion has long been in place. From the 1960s until recently 139 polders were constructed to serve as the first defence against wave actions in the coastal area. Moreover, following national land use policy, the government is planning to execute a land zoning project in the area. A total number of 301 land zones are initially identified among which 99 zones are recognised in the coastal area of the country. The LSCE model shows the areas having embankments, polders and land reclamation projects as very low to low susceptible areas to erosion in the future (see Fig. 12).

The elicitation of expert views brings a new outlook on the increasing human interventions in the coastal area of the country. The experts opined that the future intervention plans by the government in managing coastal lands might introduce a two-dimensional threat for human settlements as well as for the natural environment under changing scenarios of hydro-climatic forces in the area. Their discussion indicates that the likely impacts of Land Reclamation Project of the government could bring both positive and negative impacts on lands in the area. For instance, the proposed plan for Sandwip-Urir Char-Noakhali closures (Fig. 13) might increase prolonged waterlogging and drainage congestion problem in Noakhali coastal area. The likely reclamation of new lands would stop the south-ward natural drainage network in the area. Moreover, the impacts might aggravate the existing condition of ecology and biodiversity in the area. However, they

recommended diverting the existing channels to the eastern and western perennial channels as a probable solution to the problem but it would be economically less viable. On the other hand, the expert opined that the construction of closures connecting small islands in the area between Tetulia and Shahbazzpur channels might bring positive impacts on the stabilisation of lands and hence could reduce erosion susceptibility of lands in the area. The experts recommended assessing the controls of physical settings over the existing hydro-climatic conditions before implementing any development projects in the area. Moreover, they argued that the assessment of likely changes in hydro-climatic conditions for each project site is crucial for the entire coastal area.

The experts also opined that it would be fascinating to observe the impacts of the land-zoning project on the management of high erosion susceptible and newly accreted coastal lands in the future. They also opined that Land Reclamation Project (LRP) of the government would be a crucial issue to follow-up its effects on land dynamics and erosion susceptibility in the coastal area. The prevalence of mudflats in the central coastal zone (Fig. 14) has the potential to reclaim lands in the area.

Conclusion

This study assessed the impacts of likely changes in hydro-climate drivers on future coastal erosion susceptibility along with the underlying physical settings by applying the LSCE model in the coastal area of Bangladesh. The scenarios show

that over time a substantial amount of land in the coastal area would be inclined to high and very high erosion susceptibility. This amount would vary with the changing impacts of hydro-climatic triggering factors in the future. Additionally, considerable seasonal variations in erosion susceptibility are predicted by the model scenarios. Spatially, the western and eastern coastal zones were modelled as low to moderately susceptible whereas, the central coastal zone was identified as moderate to high and very high erosion susceptibility. The islands and newly accreted lands in the central coastal zone were modelled as highly susceptible to erosion for all of the three future time-slices. The outputs of the model justified the assumed influences of likely changes in hydro-climatic drivers on future erosion susceptibility.

The model scenarios of increasing amounts of susceptible lands in the future might be a matter of great concern for the densely populated coastal area of the country. However, the generated future scenarios could offer coastal managers and policymakers insights into the nature of future physical erosion susceptibility for the entire coastal area. The outputs of this study might be helpful for future development projects and resettlement plans of the government. Future land-zoning projects of the government would also be benefited since the identification of the nature of future erosion susceptibility of the coastal area has now been accomplished by this study. More importantly, the century-long ‘Delta Plan 2100’ of the government might be advanced by the inclusion of the modelled results in the plan. This study recommends to include more scenario data to allow further analysis of seasonal variability of physical erosion susceptibility. The application of the LSCE model would be of great importance in assessing the likely impacts of hydro-climatic drivers for similar dynamic coastal areas around the world.

Acknowledgements The current research is a part of doctoral thesis at the University of Leeds, UK. The authors are thankful to the University of Leeds for funding the research under Leeds International Research Scholarships (LIRS) scheme.

Funding information The research was funded by the University of Leeds under Leeds International Research Scholarships (LIRS) scheme.

Compliance with ethical standards

The study followed ethical standards of the University of Leeds, UK.

Conflict of interest The authors declare that they have no conflict of interest.

Ethical approval The research obtained ethical approval from the University of Leeds, UK.

Informed consent All the authors are rightly informed about the submission of the paper.

Open Access This article is licensed under a Creative Commons Attribution 4.0 International License, which permits use, sharing, adaptation, distribution and reproduction in any medium or format, as long as you give appropriate credit to the original author(s) and the source, provide a link to the Creative Commons licence, and indicate if changes were made. The images or other third party material in this article are included in the article's Creative Commons licence, unless indicated otherwise in a credit line to the material. If material is not included in the article's Creative Commons licence and your intended use is not permitted by statutory regulation or exceeds the permitted use, you will need to obtain permission directly from the copyright holder. To view a copy of this licence, visit <http://creativecommons.org/licenses/by/4.0/>.

References

- Ahmed A, Drake F, Nawaz R, Woulds C (2018a) Where is the coast? Monitoring coastal land dynamics in Bangladesh: an integrated management approach using GIS and remote sensing techniques. *Ocean and Coastal Management* 151:10–24. <https://doi.org/10.1016/j.ocecoaman.2017.10.030>
- Ahmed A, Nawaz R, Drake F, Woulds C (2018b) Modelling land susceptibility to erosion in the coastal area of Bangladesh: a geospatial approach. *Geomorphology* 320:82–97. <https://doi.org/10.1016/j.geomorph.2018.08.004>
- Ahmed A, Woulds C, Drake F, Nawaz R (2018c) Beyond the tradition: using fuzzy cognitive maps to elicit expert views on coastal susceptibility to erosion in Bangladesh. *Catena* 170:36–50. <https://doi.org/10.1016/j.catena.2018.06.003>
- Akhter, F, Mahmud, F (2007) A study on erosion and accretion of the main islands in the Meghna Estuary. B.Sc. Engg. Thesis, Dept. of Water Resources Engineering, BUET, Dhaka
- Alexandrakis G, Karditsa A, Poulos SE, Ghionis G, Kampanis NA (2010) Assessment of the vulnerability to erosion of the coastal zone due to a potential rise of sea level: the case of the Hellenic Agent Coast. In: *Environmental Systems*. Achim S ed. United Nations Educational Scientific and Cultural Organization (UNESCO) in partnership of Encyclopedia of Life Support Systems (EOLSS), vol. 3
- Ali A, Mynett AE, Azam MH (2007) Sediment dynamics in the Meghna estuary, Bangladesh: a model study. *Journal of Waterway Port Coastal and Ocean Engineering* 133(4):255–263
- Banglapedia (2018) National encyclopaedia of Bangladesh. Asiatic Society of Bangladesh, Dhaka
- Bangladesh Agricultural Research Council [BARC] (2017) Land Resources Information and Maps of Bangladesh. <http://maps.barcapps.gov.bd/index.php>. Accessed 10 March 2017
- Bangladesh Bureau of Statistics [BBS] 2015. Population monograph of Bangladesh, Population density and vulnerability: a challenge for sustainable development of Bangladesh, volume 7
- Bangladesh Inland Water Transport Authority [BIWTA] (2017) Department of hydrography, Bangladesh inland water transport authority, Dhaka, Bangladesh
- Bangladesh Meteorological Department [BMD] (2016) Climate Data Portal. <http://bmd.wowspace.org>. Accessed 25 October 2016
- Brammer H (2014) Bangladesh's dynamic coastal regions and sea-level rise. *Clim Risk Manag* 1:51–62
- Brown S, Nicholls RJ, Lázár AN, Hornby DD, Hill C, Hazra S, Addo KA, Haque A, Caesar J, Tompkins EL (2018) What are the implications of sea-level rise for a 1.5, 2 and 3 °C rise in global mean temperatures in the Ganges-Brahmaputra-Meghna and other vulnerable deltas? *Reg Environ Chang* 18(6):1829–1842

- Bangladesh Water Development Board [BWDB] (2016) Processing and flood forecasting circle, Hydrology Section, Dhaka, Bangladesh
- Centre for Climate Change Research [CCCR] (2016) CORDEX South Asia Multi Model Outputs. <http://cccr.tropmet.res.in>. Accessed 15 February 2016
- Climate Change Knowledge Portal [CCKP] (2016) World Bank. <http://sdwebx.worldbank.org/climateportal>. Accessed 20 February 2016
- Centre for Environmental and Geographic Information Services [CEGIS] (2014) Using GIS tools & rapid assessment techniques for determining salt intrusion. Centre for Environmental and Geographic Information Services, Dhaka, Bangladesh
- Crosetto M, Tarantola S (2001) Uncertainty and sensitivity analysis: tools for GIS based model implementation. *Int J Geogr Inf Sci* 15(5):415–437. <https://doi.org/10.1080/13658810110053125>
- Crosetto M, Tarantola S, Saltelli A (2000) Sensitivity and uncertainty analysis in spatial modelling based on GIS. *Agriculture Ecosystems and Environment* 81:71–79
- de Smith MJ, Goodchild MF, Longley PA (2018) Geospatial analysis a comprehensive guide to principles techniques and software tools. Leicester, Troubador Ltd
- Environmental Systems Research Institute [ESRI] (2018) Standard classification schemes. [Online]. [Accessed 19 November 2018]. Available from: <http://webhelp.esri.com>
- Fitzgerald DM, Fenster MS, Argow BA, Buynevich IV (2008) Coastal impacts due to sea-level rise. *Annu Rev Earth Planet Sci* 36:601–647
- Global Multi-Resolution Topography [GMRT], 2017. Bathymetry. <https://www.gmrt.org>. Accessed 16 January 2017
- Huq S, Karim Z, Asaduzzaman M, Mahtab F (1999) Vulnerability and adaptation to climate change for Bangladesh. Springer, Dordrecht
- Intergovernmental Panel on Climate Change [IPCC] (2007a) Climate change, impacts, adaptation and vulnerability. Contribution of working group II to the fourth assessment report of the intergovernmental panel on climate change. In: Parry ML, Canziani OF, Palutikof JP, van der Linden PJ, Hanson CE eds. Intergovernmental Panel on Climate Change (IPCC). Cambridge University Press, New York
- Intergovernmental Panel on Climate Change [IPCC] (2007b) AR4, fourth assessment report: climate change 2007. Intergovernmental panel on climate change
- Intergovernmental Panel on Climate Change [IPCC] (2014) AR5, fifth assessment report: climate change. Intergovernmental panel on climate change
- Islam MSN (2008) Cultural landscape changing due to anthropogenic influences on surface water and threats to mangrove wetland ecosystems: a case study on the Sundarbans, Bangladesh. Dissertation, Brandenburg University of Technology, Cottbus
- Institute of Water and Flood Management [IWFM] (2012) Component 3: study on residual flow in the Bay of Bengal considering future climate change induced hydro-meteorological scenarios. Project report, Climate Change Study Cell, 1–36
- Kamal R, Matin MA, Nasreen S (2013) Response of river flow regime to various climate change scenarios in Ganges-Brahmaputra-Meghna basin. *Journal of Water Resources and Ocean Science* 2(2):15–24
- Kay S, Caesar J, Wolf J, Bricheno L, Nicholla RJ, Islam AKMS, Haque A, Paradaens A, Lowe JA (2015) Modelling the increased frequency of extreme sea levels in the Ganges-Brahmaputra-Meghna delta due to sea level rise and other effects of climate change. *Environmental Science* 17:1311–1322
- Mahmood SAI (2012) Impact of climate change in Bangladesh: the role of public administration and government's integrity. *Journal of Ecology and the Natural Environment* 4(8):223–240
- Masselink G, Russell P (2013) Impacts of climate change on coastal erosion. *MCCIP Science Review* 71–86
- Ministry of Environment and Forests, Bangladesh [MoEF] (2007) Bangladesh: National Programme of Action for Protection of the Coastal and Marine Environment from Land-Based Activities. <http://www.doebd.org>. Accessed 15 July 2016
- Ministry of Environment and Forests [MoEF] (2016) Assessment of sea level rise on Bangladesh coast through trend analysis, Climate Change Cell, Department of Environment, Government of the Peoples' Republic of Bangladesh
- Ministry for Primary Industries [MPI] (2017) Plantation forestry Erosion susceptibility classification: risk assessment for the National Environmental Standards for Plantation Forestry, MPI Technical – Paper No: 2017/47, New Zealand
- Naylor LA, Stephenson WJ, Trenhaile AS (2010) Rock coast geomorphology: recent advances and future research directions. *Geomorphology*. 114:3–11
- Pannell DJ (1997) Sensitivity analysis: strategies, methods, concepts, examples. *Agric Econ* 16:139–152
- Permanent Service for Mean Sea Level [PSMSL] (2017) Obtaining tide gauge data. <http://www.psmsl.org>. Accessed 11 January 2017
- Ramieri E, Hartley AB, Filipe DS, Ana G, Mikael H, Pasi L, Natasha M, Monia S (2011) Methods for assessing coastal vulnerability to climate change. ETC CCA Technical Paper, European Environment Agency
- Sarrazin F, Pianosi F, Wagener T (2016) Global sensitivity analysis of environmental models: convergence and validation. *Environ Model Softw* 79:135–152
- Saunders W, Glassey P (2007) Guidelines for assessing planning policy and consent requirements for landslide prone land. GNS Science Miscellaneous Series 7
- Shibly MA, Takewaka S (2012) Morphological changes along Bangladesh coast derived from satellite images. *Proc. of Coastal Engineering*. JSCE 3:41–45
- University of Hawaii Sea Level Centre [UHSLC] (2017) University of Hawaii Legacy Data Portal. <https://uhslc.soest.hawaii.edu>. Accessed 22 June 2017
- United Nations Development Programme [UNDP] (2004) Reducing disaster risk: a challenge for development, New York: Bureau for Crisis Prevention and Recovery
- United States Geological Survey [USGS] (2001) Digital geologic and geophysical data of Bangladesh. <http://pubs.usgs.gov>. Accessed 17 August 2016
- United States Geological Survey [USGS], 2017. Digital Elevation Model. <https://earthexplorer.usgs.gov>. Accessed 20 January 2017
- Van RLC (2011) Coastal erosion and control. *Ocean Coast Manag* 54: 867–887. <https://doi.org/10.1016/j.ocecoaman.2011.05.004>
- Viles H, Spencer T (1995) Coastal problems. Taylor and Francis, London
- Water Resources Planning Organization [WARPO] (2018) Mudflats in the coastal area of Bangladesh. National Water Resources Database (NWRD), Ministry of Water Resources, Government of the People's Republic of Bangladesh
- Warrick RA, Ahmad OK (eds) (1996) The implications of climate and sea-level change for Bangladesh. Kluwer Academic Publishers, Dordrecht

Publisher's note Springer Nature remains neutral with regard to jurisdictional claims in published maps and institutional affiliations.